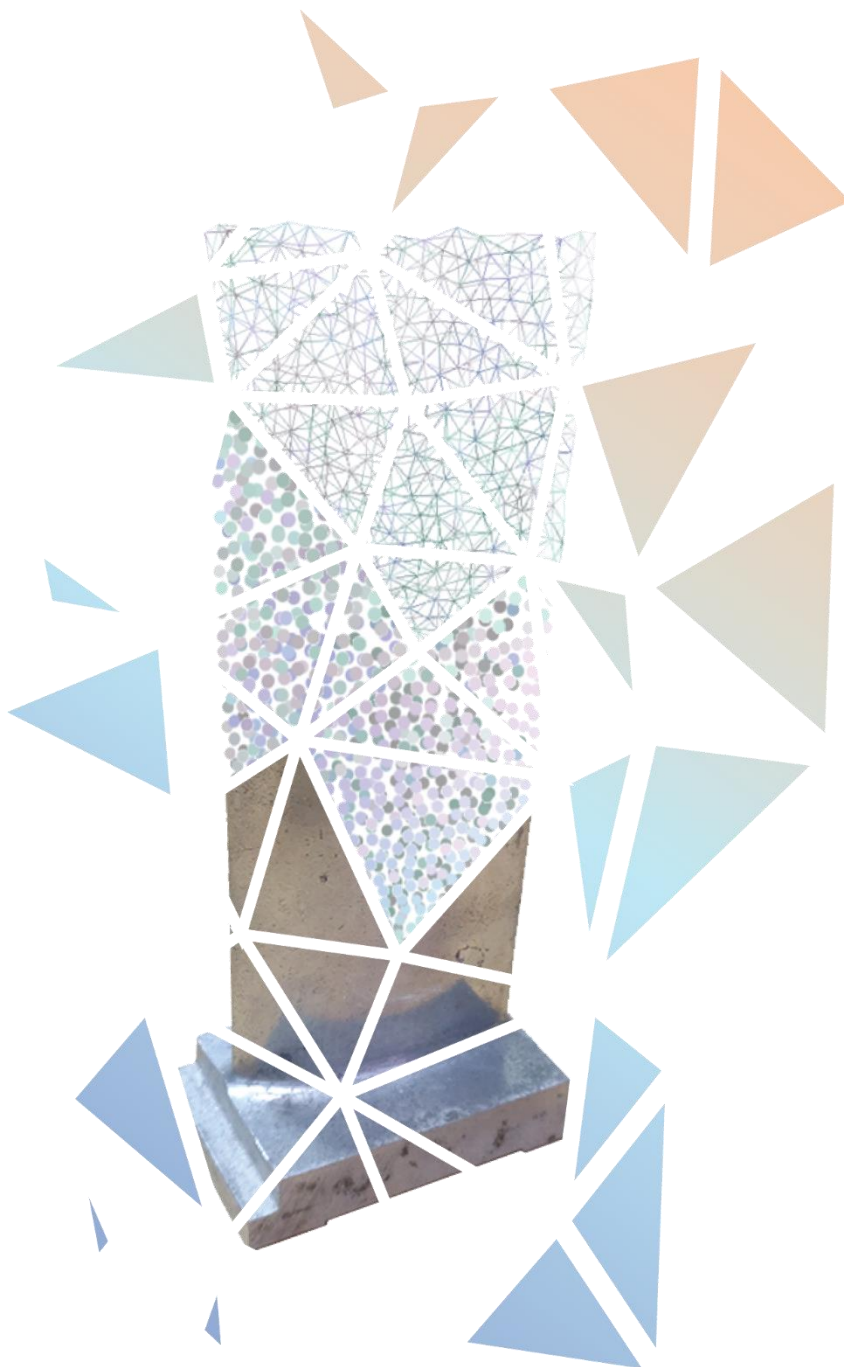

DYNOSCAN 3D



GROUP 7

AHMED AZEEM
CHUAN SHENG TIONG
HUSSAIN SIDDIQUEY
JEREMY TAN
SIEW HAN LIM

SUPERVISORS

DR LOIC SALLES
DR CHRISTOPH
SCHWINGSHACKL

3 JUNE 2020
80 PAGES

1 Executive Summary

Imperial College London's Dynamics group is involved in the analysis of engine components, such as turbine blades, which requires accurate 3D models. Based on the requirements of the Dynamics group, commercial solutions are either too expensive or generate 3D models that are not of a desired accuracy. 3D Dynoscan aims to bridge this market gap by providing a low-cost, portable, and modular scanning solution that produces 3D models accurate to a resolution of 0.5 mm.

3D Dynoscan can be divided into three critical components: a turntable subassembly, a scanning system, and an electrical controls system. The turntable subassembly consisted of a 4:1 belt-pulley transmission which connected a permanent magnet stepper motor and a 500 mm diameter aluminium turntable. Its purpose was to rotate the object that was to be scanned, in small rotational increments, such that a complete 3D model could be constructed. The extent of angular rotation was controlled by an Arduino Uno and Pololu A4988 Driver Carrier with direct control. The scanning system utilises Structured Light Scanning technology and consists of a Logitech C920 webcam and an AAXA P300 Neo projector, mounted on a modified camera tripod that allows for pitch and height control, which may be adjusted based on the size of the object that is being scanned.

Due to the unforeseen circumstances caused by COVID-19, which resulted in early college closure, the last week of term that was reserved for final product testing was unable to be carried out. Consequently, an Alternative Work Package was undertaken to investigate the effects of surface and environmental conditions on the scan quality.

However, prior testing has shown the ability for the independent scan components to produce a 3D object in the required file formats. Furthermore, the overall system was easily portable by two people and each individual scan took at most 90 seconds, excluding the time taken for processing of the point cloud files. Thus, the three initial requirements of this project have been satisfied.

While Dynoscan 3D has achieved its initial objectives, it can be further improved by integrating an automated point cloud alignment process as currently it is a tedious and manual process. Ideally this automated process would leverage an Iterative Closest Point algorithm to stitch the point cloud files together. Furthermore, including an additional camera to the scanning system would improve scan times and scan accuracy. Lastly, the material selection for the frame could be optimised to reduce costs, as it is a non-load bearing structure.

2 Contents

1	Executive Summary.....	2
3	Introduction and Background	5
4	Project Context.....	7
4.1	Justification of Product Design Specification (PDS)	7
4.2	Project Objectives - PDS	8
4.3	Market Research.....	10
4.4	Literature Review.....	11
4.5	Project Timeline.....	14
5	Project Organization	14
5.1	Group Roles.....	14
5.2	Design Principles and Management	15
6	Concept Development	15
6.1	Development Priority	15
6.2	Scanning Method	15
6.3	Hardware	17
7	Prototype Development	18
7.1	Prototype Considerations.....	18
7.2	Turntable Subassembly	18
7.3	Scanner	25
7.4	Control.....	29
8	Prototype Testing	30
8.1	Turntable.....	30
8.2	Scanner	38
9	Evaluation of Prototype	46
9.1	Summary of Prototype Tests Results.....	46
9.2	Evaluation of Structural Integrity Test	47
9.3	Evaluation of Electrical Controls Test.....	48
9.4	Scanning Considerations	49
10	Design Iteration and Further Development.....	49
10.1	Design Considerations.....	49
10.2	Transmission	50
10.3	Scanner Mount	51
10.4	Lighting Control	53
10.5	Electronics.....	53
10.6	Encapsulation and Covers.....	56
10.7	Additional Changes	58

11	Manufacturing	58
12	Final Design	59
12.1	Scanning Assembly.....	59
12.2	Transmission Assembly	60
12.3	Overall Assembly	62
12.4	Engineering Analysis	63
13	Project Budget	65
14	Alternative Work Package	65
14.1	Background	65
14.2	Considerations.....	67
14.3	Methodology	67
14.4	Results	68
14.5	Analysis and Discussion.....	69
15	Future Improvements	71
16	Conclusion.....	72
17	References	73
18	Individual Reflections.....	75
18.1	Siew Han	75
18.2	Ahmed Azeem.....	76
18.3	Jeremy Tan	77
18.4	Hussain Siddiquey	78
18.5	Chuan Sheng Tiong.....	79

3 Introduction and Background

Imperial College London's Dynamics Group has research interests in the analysis of small to medium-sized turbine engine components, which consists of hundreds of smaller elements with irregular geometry such as turbine blades. In order to perform vibrational, stress and other detailed analysis on these components, a complete 3D model is often required. While the engineering drawings are available from which 3D CAD models can be constructed manually, this is often a time consuming and error prone process as the drawings are decades old and difficult to read. Market research, in Section 4.3, revealed that existing commercial solutions were not suitable for the needs of the Dynamics Group. The existing solutions were either prohibitively expensive as they exceeded the agreed budget of £1000, were unable to achieve a scan accuracy of less than 0.5 mm or were incompatible with large or heavy objects. For the purposes of this report, scan accuracy refers to how close the digital dimensions of a scanned object measure up to its real-life counterpart.

Consequently, a 3D scanning device was requested by the Dynamics Group to streamline the process of creating 3D CAD models of engine components. For accurate analysis of engine components, the following requirements for the developed 3D scanning solution were stipulated at the start of the project:

1. Dimensions of the 3D CAD models must be accurate to 0.5 mm when compared to the real object
2. 3D Scanner must be able to scan objects weighing up to 20 kg, 300 mm in length and 500 mm in diameter
3. 3D Scanner must be modular allowing for future upgrading of hardware and be portable by 2 people or fewer

Due to the unforeseen circumstance of COVID-19, Imperial College London's campuses were closed prematurely on 18 March 2020 and the final product was submitted on this effective date. As a result, the last week of Spring Term that was scheduled for testing of the complete final product was cut short and tests could not be conducted. As agreed with the project supervisors Dr Schwingshackl and Dr Salles, an Alternative Work Package of a similar scope and time commitment of the original testing plan, was required to compensate for the lack of final product testing. Further details of the Alternative Work Package, which consists of conducting further scan tests to optimise scan quality based on ambient lighting conditions and surface treatment conditions, will be explained in greater detail in Section 14.

This report encapsulates the design journey of the Dynoscan 3D project, featuring the iterative design process and justifications for particular design decisions. The Introduction and Background of this report serve to provide the context behind the need for a 3D scanner. In

the Project Context section, the formal requirements of the 3D scanner are stipulated in the Product Design Specification as well as background research of commercial products and the basic operating principles of various scanning methods. The bulk of the design journey is captured in the Concept Development and Prototype Development sections. Subsequently, the test results of the prototype are discussed and evaluated against the PDS. From this initial analysis, the lessons learned from developing the prototype are applied to the next iteration until the final model was developed. The expenditure is broken down in the budget section and the results of the Alternative Work Package are discussed. Future improvements are highlighted in the event of this project's continuation, and a brief conclusion ends this report. Lastly, individual reflections on how the project went are appended at the end of the report.

4 Project Context

4.1 Justification of Product Design Specification (PDS)

Based on the first project requirement stated in the prior section, it was decided that the scanner should output the model in a 3D modelling file that is accessible through commercially available software such as Solidworks, which is used by Imperial College London's Dynamics Group. A resolution of 0.5 mm was chosen both by surveying commercial scanners at the project's budget range and discussing with the Dynamics Group for the tolerances required of scanned objects.

In order to address the second project requirement, the design must be light enough for two people to transport over a short distance. A study by Karwowski (1) showed that for a pair of males and females, 95% of the human population are incapable of lifting loads greater than 83 and 63 kg, respectively. Consequently, the lower bound of 63 kg was taken and a safety factor of 2 was applied to reach a 30 kg maximum weight threshold for the product to be comfortably transported.

Since future iterations and improvements of the scanning device are plausible, the design should accommodate for a modular scanning device housing and facilitate the ease of integration.

Calibration is required to determine the intrinsic and extrinsic parameters of any optical device, to obtain an accurate and complete replication of object. To facilitate ease of use, this procedure should be done as infrequently as possible, ideally only when the positions of the optical devices such as the camera and projector are moved relative to each other.

Environment and operating conditions must be considered as it may affect scan quality. As the Dynamics lab is a closed environment, variable lighting conditions can be achieved, such as having a dark room or one that is brightly illuminated (2).

The Product Design Specification in the following subsection shows a detailed list of objectives, verification plan, and the current status as of project submission. Under the status column, green indicates that the object is fulfilled, while yellow indicates a lack of testing.

4.2 Project Objectives - PDS






Aspect	Objective	Quantitative Measure	Verification	Status
Technical Requirements				
Scan Volume	Able to scan engine components of the Dynamics group	Maximum object size of Ø500 mm diameter and 300 mm height. Able to support objects up to 20 kg	Review of design and mechanical load testing of the turntable	
3D Model Resolution	Scanner should be able to capture minute details in the objects	Point cloud resolution of less than 0.5 millimetres	Compare 3D model dimensions to the object's real dimensions	
Scanning Software	Software must be accessible and modifiable without any prior purchase.	-	-	
Modularity	Scanning devices should be installed in a modular manner to accommodate for future improvements.	-	-	
Operation				
Scanner Output	Data must be taken from the object from all angles and preferably stored in a suitable 3D modelling format.	Output of point cloud in '.ply' format and mesh in '.stl'	-	
Scanning Device Position	Scanning device to be adjustable with respect to the platform in order to optimise scan results.	-	Review of design	
Scan time	Scanning should not take an excess amount of time	Scan time of less than an hour	Record operational time	
Environment	Scanner to be operated in the Dynamics laboratory	Able to run at ambient conditions and lighting	Operate scanner in various lighting conditions	
Mass	The scanner should be portable by two people	Mass of less than 30kg, the comfortable carrying load for two persons (2)	Physically weigh the completed product	
Transportability	The scanner should be portable by two people	NA	Review of user feedback	
Life				
Service Life	Scanner should last long enough for customer to make further modifications and upgrades.	Service life of at least 5 years	Calculation of service life of parts under stress	
Maintenance	Scanning device and housing must be accessible for maintenance	-	Review of design	
Production				
Costs	Total costs including prototyping to be under £1000. Additional funds up to £1000 may be given to procure a more expensive optical scanning device.	-	Review of expenditure sheet	
Safety and Standards				
Drawing Standards	BS 8888	-	-	

Lab Safety Standards	No exposed wiring and transmission parts as well as electrical short circuits	-	Electrical schematics to be verified by technician Mr. Leroy Grey	
Setup Safety	The user should be informed of the device's current operational state	Clear indication of machine state	-	
Operational Safety	Should the user deem the operation unsafe, means of immediate termination should be provided	Failsafe switch to kill operation	Testing of failsafe switch in various stages of operation	
Mechanical Safety	No exposed sharp edges to minimise injuries whilst handling product.	-	Review of Design and physical inspection	

4.3 Market Research

Research into commercially available 3D scanning devices was conducted, and summarised in Table 1, in the event that a scanning device, that met the PDS requirements, could be integrated into a larger scanning system. This would eliminate the need to independently create one and therefore more resources could be redirected to the mechanical aspect of the project.

Table 1 Summary of the advantages and disadvantages of commercial solutions.

Scanner	Advantages	Disadvantages
 <p>EORA 3D Scanner</p> <p>Smartphone-based laser scanner (3)</p>	<p>£455</p> <p>Resolution of ≈ 0.1 mm</p> <p>High point cloud density</p> <p>Weighs 2.2 kg</p>	<p>Proprietary software</p> <p>Turntable max load of 5 kg</p> <p>Maximum scan size of 300 mm in diameter</p> <p>Poor generation of watertight mesh</p> <p>Turntable only rotates in 10 increments</p> <p>Relies exclusively on smartphone and app interface</p>
 <p>Matter and Form</p> <p>Laser scanner with built in turntable (4)</p>	<p>£570</p> <p>Resolution of ≈ 0.1 mm</p> <p>Weighs 1.71 kg</p>	<p>Proprietary software</p> <p>Maximum scan size of 250x180 mm</p> <p>Turntable max load of 3 kg</p>
 <p>Einscan-SE 3D Scanner</p> <p>Structured Light Scanner (5)</p>	<p>Point distance resolution of 0.17-0.2 mm</p> <p>High point cloud density</p> <p>Weighs 4.9 kg</p> <p>Can operate without turntable</p> <p>Scan time of 4 – 60 seconds</p>	<p>Proprietary software</p> <p>Turntable max load of 5 kg</p> <p>> £1,400</p>
 <p>Peel 3D Scanner</p> <p>Handheld Structured Light Scanner (6)</p>	<p>Point distance resolution of 0.5 mm</p> <p>Weight 0.95 kg</p>	<p>Proprietary software</p> <p>> £5,900</p>
 <p>GOM – ATOS Scanbox 4</p> <p>Structured Light Scanner (7)</p>	<p>Point distance resolution of 0.05 mm</p> <p>Industrial solution</p>	<p>Proprietary software</p> <p>> £100,000</p>

After evaluating the existing commercial products, several areas for possible improvement were identified, such as allowing for rotational control of the turntable mechanism. For example, EORA 3D Scanner's turntable could only rotate in increments of 10 (36° each step). Generally, it is desirable to be able to increase the number of rotational increments of a turntable, as it allows for more details to be captured and hence a more accurate model to be constructed. Several of the commercial solutions had small turntables that were made from plastic, which would not support a 20 kg or objects larger than 500 mm in diameter. Lastly, all the commercial solutions utilised proprietary software, which did not allow the user access to the code. This restricts the extent to which the scanning device can be upgraded or modified to suit various scanning needs.

As such, a self-made scanning device system was required as none of the commercial solutions met the requirements stipulated by the PDS. The available methods of 3D data acquisition can be divided into Structured Light Scanning, Laser Triangulation, Flash LIDAR (Time of Flight), and Photogrammetry, which are discussed in Section 4.4 and the merits of each method are evaluated in Section 6.2.

4.4 Literature Review

4.4.1 Structured Light

Structured Light scanning utilises a setup that features at least one projector and one camera to obtain data about the 3D geometry of an object. This is commonly achieved by projecting a series of patterns onto an object, which distorts based on the object's shape. This distortion of the projected patterns is captured by the camera and processed by software to output a point cloud file, which contains the discretised data points of the object's geometry in 3D space. For a projector and camera to be used in a Structured Light configuration, they both need to be calibrated to accommodate for how the camera and projector are positioned relative to each other. This calibration process is essential in mapping each of the camera's pixels to the projector so that an accurate 3D point cloud file can be created via triangulation (8).

However, the quality of the point cloud file is limited by the camera and projector resolution. As such, it is not possible to attain pixel level resolution as the projected black and white stripes are typically of a larger size than the individual pixels themselves.

Structured Light is commonly used for quality assurance in manufacturing to identify defective surface geometry, 3D reconstruction of remote environments such as submarine terrain and underground tunnels, and reverse engineering of objects with complex geometry (9).

4.4.2 Flash LIDAR (Time of Flight)

LIDAR stands for light detection and ranging, where light is projected as a pulse which illuminates the desired environment and reflects off objects and returns to the LIDAR sensor, producing a range map of the environment. Flash LIDAR functions like a commercial 2D camera as it can record the position of objects and their respective light intensity in its field of view, but is also able to capture the depth of objects by using the time taken for the emitted light pulse to return to the sensor (10).

The Flash LIDAR systems consist of a lens, an integrated light source, a sensor, and an interface. The LIDAR sensors usually consist of a Charge Coupled Device (CCD) that can store the data. The emitted light can take the form of a singular pulse or a continuous light wave. The speed of light and the time taken for the pulse to return to the sensor are used to calculate the distance of objects. For an integrated light source that emits continuous light waves, the phase shift between the outgoing and incoming light waves is used to measure the distance of the object (11).

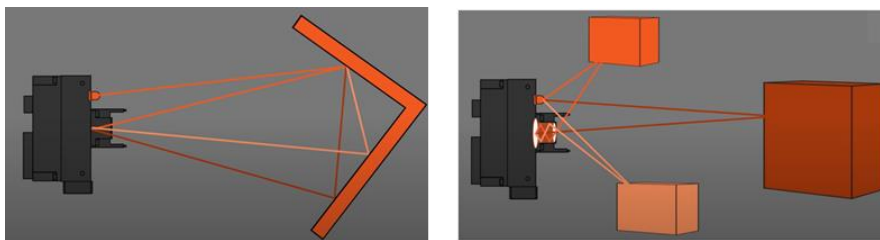


Figure 1 Effects of corner geometry and overexposure of nearby objects (10).

Flash LIDAR operates on the principle that the emitted light is only reflected once, and as a result, objects with complex geometry featuring corners or concave shapes will cause distortions on the recorded data shown in Figure 1. Operation in strong ambient light will also cause the sensor to be oversaturated with stray light. Similarly, nearby objects that are brightly illuminated will reflect light back into sensor causing overexposure which will cause distortions in the stored data.

4.4.3 Laser Triangulation

Laser triangulation utilises trigonometry to calculate the depth of a point as well as its position. Certain parameters of the instrumentation set up must be known such as the camera field of view, camera angle, camera-laser distance, and laser angle, in order for the x, y and z coordinates to be computed.

In order to obtain a complete 3D scan of an object, a point or line laser is projected onto an object. Line lasers can cover more of the surface area of the object at a time during scanning

compared to point lasers, which results in a reduced scan time. The object must rotate relative to the laser scanner to ensure all angles of the object are covered. This is usually accomplished by rotating the object and keeping the scanner stationary or vice versa. During the data acquisition process, if the object or scanner is rotating at fixed speed, the data sampling can be carried out at regular intervals. However, if the rotational speed is constantly changing, a rotational encoder may be required to establish correspondence between the sampled data and the position of the rotating object (12).

4.4.4 Photogrammetry

Photogrammetry is able to construct a 3D profile by analysing photos of the same object from different angles and using triangulation to determine the depth profile of the object. This can be accomplished with a multiple camera set up or a single camera that changes position to capture different angles of the object. The captured photos must have overlapping features to use as a common reference during analysis via triangulation, similar to the Laser Triangulation process in Section 4.4.3.

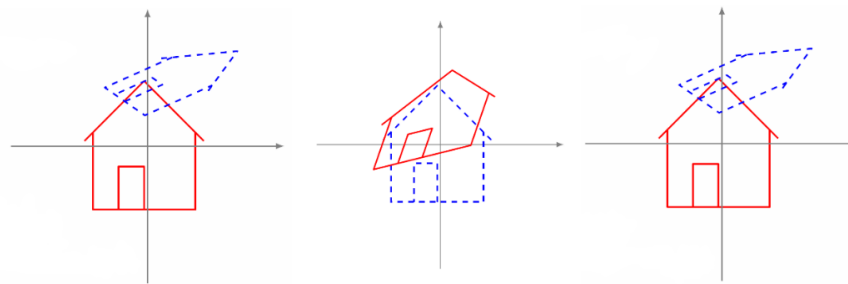


Figure 2 Rigid body, affine, and perspective transformations respectively (13).

During the analysis of the photos taken, three main transformations are applied to the acquired data illustrated in Figure 2. Rigid body transformations either scale, translate, or rotate an image. Rigid body transformations preserve all geometric angles and hence the overall shape of the image. Affine transformations rotate and/or scale the image, which results in the parallelity of the shape being preserved but not the angles. Projective transformations effectively show how the image changes when the viewer's perspective changes. Neither angles nor parallelity are preserved in this transformation. Each of these transformation types have their own unique transformation matrix and can be used to correct for the different perspectives of the images taken.

4.5 Project Timeline

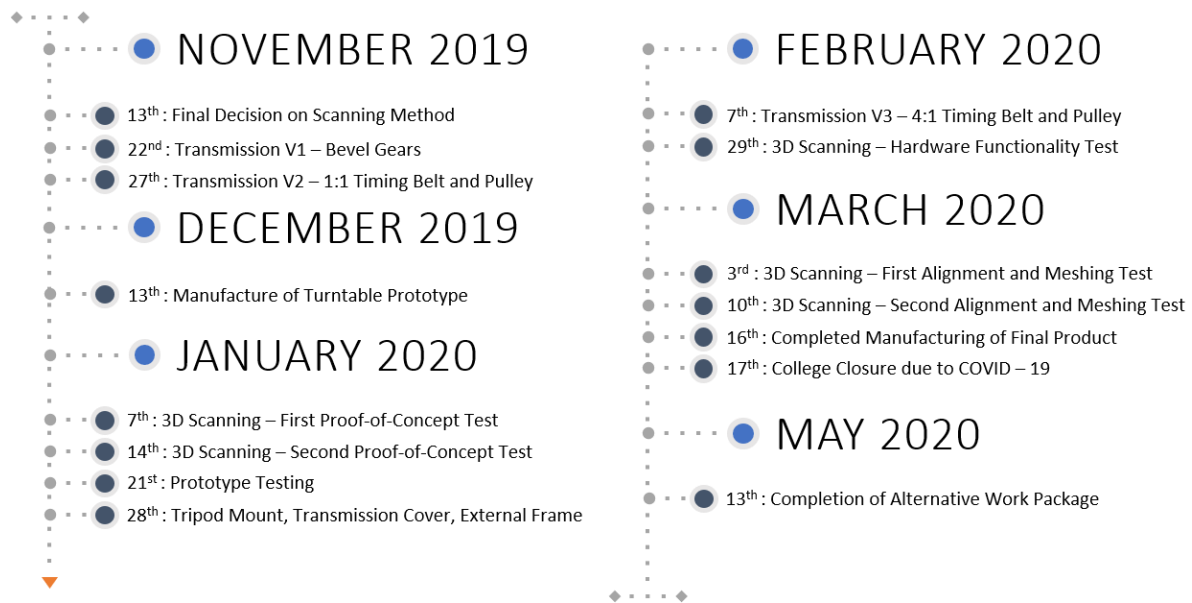


Figure 3 Timeline depicting key project milestones

The above Figure shows key internal milestones of the project. It is noted that all activities after March the 17th were curtailed due to college closure, with the exception of the Alternative Work Package.

5 Project Organization

5.1 Group Roles

The roles and responsibilities of each group member are summarised in Table 2.

Table 2 Summary of roles and responsibilities of each team member.

Name	Role	Responsibilities
Jeremy Tan	Deadline Manager	Ensures deadlines are met, identify dependency events and plan lead time.
	Project Manager	Sets overall direction for the project and monitors progress.
Siew Han Lim	Report Manager	Oversees the outline of the report. Ensures consistency in format and work done.
	Document Control	Organise project documents on Microsoft Teams/repositories.
	Software Lead	Develop code and adapt resources to implement the 3D scanning procedure.
Chuan Sheng Tiong	Team Liaison Officer	Group liaison for project supervisors and meetings with staff. Disseminate supervisor meeting minutes.
	CAD Manager	Oversees modelling and engineering drawing process, ensuring communication between members for coherent work.
	Electronics and Control Lead	Oversees motor control and other relevant electronic integration.
Ahmed Azeem	Budget Manager	Tracks expenditures associated with the project to minimise costs.
	Procurement Manager	Sources for appropriate commercial components as well as raw material for manufacturing.
	Manufacturing Lead	Sets out the manufacturing plan based on team capabilities, ensuring prerequisites like engineering drawings are up to date.
Hussain Siddiquey	Administration and Minutes	Keeps a log of minutes from all meetings, and book appropriate workspaces when needed.
	Analysis Lead	Discerns relevant areas requiring performance and structural analysis.

5.2 Design Principles and Management

An AGILE-style approach was applied to the project management and design aspect of this project, particularly because the project was not linear in scope. Development on software and hardware had to occur simultaneously whilst being revised regularly to ensure continuous improvement, with the software and other documents stored on GitHub for version control, accessed at <https://github.com/DynoScan3D>. The project was broken down into several large tasks and prioritised in order of importance. Iterations of concepts and designs were evaluated weekly with the guidance of the supervisors to ensure user feedback was integrated into the design.

6 Concept Development

6.1 Development Priority

Development of the scanner required careful consideration of many aspects related to mechanical design, transmission, electronics, and software. The type of scanning method was deemed the most critical design aspect as all other components were dependent on this and changing the scanning method would have resulted in a complete overhaul of the design.

After the scanning method was chosen, only then could the transmission be selected since the scanner could be more depicted more accurately based on the requirements of the optical components. Following this, mechanical components would be designed to support the overall structure along with relevant electronics given the spatial constraints.

6.2 Scanning Method

The selection of the scanning method was considered to be the most important stage of the design process as the scanner required a high resolution despite the manufacturing limitations inherent in a student workshop and while maintaining portability and ease of use. Following a literature review and market research, as described in Section 4, four methods were considered the most viable. Table 3 summarises the advantages and disadvantages for each of these methods.

Table 3 Comparison of each scanning method.

Scanning Method	Advantages	Disadvantages
Time-of-flight Laser swept across a rotating object	Data processing is relatively fast and simple given a known turning revolution and capture frequency rate	Requires either the laser or object to be moving with known trajectory during scanning procedure, requiring high tolerance on manufactured components for smooth movements and precise speed control
	Simple equipment setup with no calibration needed	Poor sensor depth accuracy (± 5 mm for a £200 laser (14))
		Object needs to be repositioned to scan top and bottom

Structured Light Scanning	Resolution limited by camera and projector resolution, thus able to be improved	Cannot operate correctly in bright ambient lighting due to optical noise
		Requires two separate motors for the laser and the object
		Shiny or transparent objects could distort patterns unreliably, preventing accurate scanning
		Calibration process required before scanning
Laser Triangulation swept across an object	Can use slit laser to reduce scan time	Relatively more complicated to reconstruct a 3D point cloud from captured data
		Requires either the laser or object to be moving with known trajectory during scanning procedure, requiring high tolerance on manufactured components for smooth movements and precise speed control
		High resolution laser sensors/probes can exceed the budget as 1D laser can cost at least £2,750 (14)
Photogrammetry	Able to reproduce images in full colour and texture	Cannot operate correctly in bright ambient lighting due to optical noise
		Generally lower resolution compared to Structured Light Scanning (15)
		Requires the object to have a unique texture for feature recognition during reconstruction, and thus struggles with smooth or symmetrical surfaces

To decide on the most suitable scanning method, the merits of each were collectively assessed on a rating scale of one to ten and averaged in Table 4 according to the following criteria:

- **Modularity:** The ease at which components can be replaced for future improvements
- **Integration:** The difficulty in obtaining and integrating the necessary open-source software and code
- **Resolution:** The scan quality of the object
- **Price:** The cost of the scan components, with ten being the cheapest
- **Implementation:** The ease in designing a mechanical system to support that scanning method

Laser triangulation was omitted since the cheapest 1D sensor was priced above the overall budget of £1000.

Table 4 Assessment of scanning methods as per weighted criteria.

Criterion [Weighting]	Time-of-Flight	Structured Light	Photogrammetry
Modularity [0.1]	5 – LIDAR components can come in 1D, 2D, and 3D variants that requires different mechanical setups	9 – Improvement by increasing projector or camera quality is easily done as operation mode does not change.	9 – Improvements by increasing camera quality easily done
Integration [0.2]	8 – LIDAR output of depth against time easily converted to 3D coordinates if trajectories and velocities are known	6 – No open source commercial software that accomplishes the whole process, requires integration of multiple resources	8 – Free open source photogrammetry software available
Resolution [0.3]	4 – Laser sensors have low resolution for budget range	8 – Generally higher resolution, used in industrial imaging solutions	6 – Lower resolution compared to structured light
Price [0.2]	9 – 1D laser sensors can cost as low as £100	7 – Wide range of commercial cameras and projectors	7 – Wide range of commercial cameras

Implementation [0.2]	3 – Requires movement in two directions (Object-sensor or sensor-sensor) for a complete surface profile to be completed	9 – Scanning carried out with stationary components and object, only needing to rotate to obtain a different viewpoint	6 – Camera needs to be rotated, and in more than one axis to obtain photographs from all angles
Score	5.7	7.7	6.3

Table 4 shows that the Structured Light Scanning method scored the highest and is therefore the optimal scanning method from the options presented. This can be attributed mainly to its high resolution and relatively low price which outweighs the difficulty of setting up the scanning process.

6.3 Hardware

Once the scanning method was selected, basic concepts for the mechanical design were then developed. One of the main decisions was the motion of the scanner relative to the object, or more simply, whether the scanner would remain stationary while the object moved and vice versa. Table 5 shows the various options that were discussed during concept development, evaluating the advantages and disadvantages of each.

Table 5 Comparison of options for relative motion between scanner and object.

Description	Advantages	Disadvantages
Robotic arm to control scanner	Can position scanner in any orientation around object	Very complicated electronics and control (beyond scope of project)
Scanner and object stationary (or both rotating)	No calibration issues	Requires manual rotation of the object otherwise only one side would be scanned
	No transmission required	
	No electronics system required	
Scanner rotates and object stationary	Rotation of the relatively light scan setup does not require much mechanical power	Risk of undoing calibration if position of camera relative to projector changes
	Can scan object from most sides	Object must be flipped over to scan the bottom side
		Vibration due to transmission and movement can potentially cause distortion of scans obtained
Object rotates and scanner stationary	Can scan object from all sides	Object must be flipped over to scan the bottom side
	Simple mechanical design	Up to a 20kg mass must be supported and rotated, requiring a strong motor and robust setup.
	No calibration issues	

The robotic arm is clearly unfeasible as it is too technically challenging and would detract attention from the original project. Keeping the scanner and object stationary was also discarded since a full body scan cannot be obtained without manual rotation of the object, which would increase scan time and make the scanning process more difficult for the user. Of the two remaining options, rotating the object while keeping the scanner stationary was the most appropriate due to its simplicity and low risk of undoing calibration since the scan components remain static throughout.

It is important to note that to scan the bottom of the object, flipping the object over is unavoidable in every option apart from the robotic arm but this has only a minor effect on the scan time and requires very little user input. The issue of rotating a 20 kg object was deemed manageable as there is no requirement for the object to be accelerated quickly, thus a motor with a high torque output would not be necessary.

7 Prototype Development

7.1 Prototype Considerations

Aims of Prototype:

1. Assess if the structural integrity of the turntable holds under maximum loading conditions
2. Determine if sufficient torque can be transmitted from the motor to rotate an object in various loading conditions
3. Determine if the motor can be controlled accurately such that rotational increments are kept constant during the scanning process
4. Assess if a scan of sufficient accuracy can be obtained

Prototype Development Context:

This section focuses on developing a prototype to test if the concepts selected in Section 6 would meet the criteria set out in the PDS. Priority was given to developing the software, turntable, and transmission rather than the electronics and other features since the scanner cannot operate correctly if any problems exist with data acquisition and processing, in which case the other features would become redundant.

7.2 Turntable Subassembly

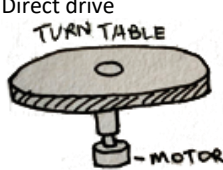
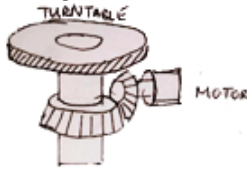
7.2.1 Transmission Ideation


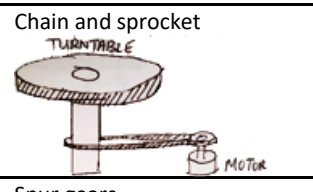
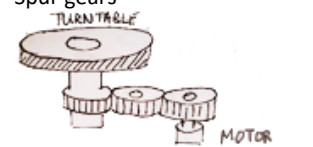
A transmission system is needed to rotate the turntable so that scans can be taken from all angles. A suitable transmission system would have the following features:

- Transmit sufficient torque from motor to turntable
- Allow compact design for portability
- Able to withstand loading from the motor, inertia of the object and friction
- Cost effective, given that a significant amount is spent on scanning components

Based on these requirements, various options were compared which can be seen in Table 6.

Table 6 Comparison of transmission systems

Transmission System	Advantages	Disadvantages
Direct drive 	No backlash of transmission for smoother movement Reduced weight Compact with fewer components	Weight of turntable/object acts directly onto the motor Can only adjust transmitted torque by adjusting power supplied to motor Large motor may be needed if significant torque required, raising the height of the turntable
Bevel gears 	Allows sideways positioning of motor, reducing turntable height Gear ratio adjustable to vary torque	Requires precise alignment for gears to mesh

	Motor placed out of turntable radius, reducing its height Transmission ratio adjustable to vary torque	Increases the width of scanner to house motor externally Requires a belt tensioner
	Motor placed out of turntable radius, reducing its height Transmission ratio adjustable to vary torque	Increases the width of scanner to house motor externally Chain and sprocket transmission costs relatively more Noisy operation
	Gear ratio adjustable to vary torque	Raises height of turntable to allow for gears Requires precise alignment for gears to mesh

7.2.2 Design Iterations

Following the discussion of each possible transmission system in Table 6, bevel gears and belt drives were selected as the most likely to fulfil the requirements set out in Section 7.2.1, as the compact transmission allowed turntable height to be fairly low while still preventing direct axial force on the motor shaft, which could damage internal components. With the aim to minimise both the turntable height and the general size of the product, two concepts were developed.

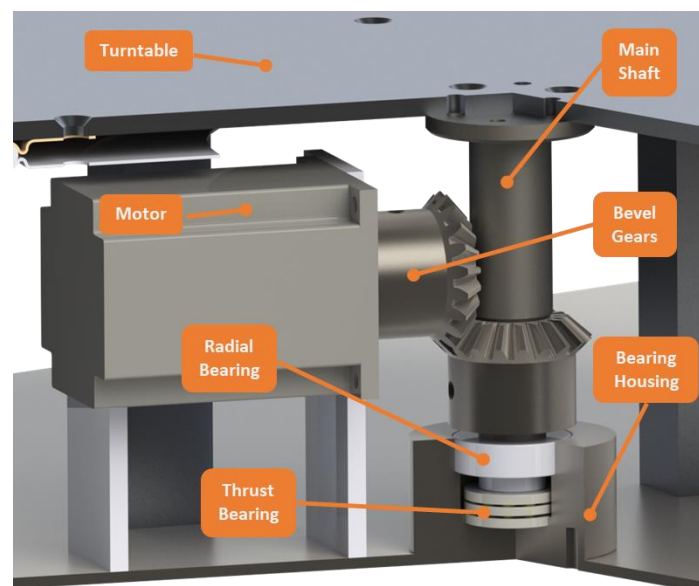


Figure 4 Section view of the bevel gear transmission design.

Figure 4 above shows the conceptualization of a bevel gear transmission system which allowed for sideways positioning of the motor. While the transmission can be contained within the turntable radius, bearing housing requirements meant that the bevel gear on the shaft was teeth facing up to prevent interference, requiring the motor to be elevated and increasing

the overall height. This resulted in a base-to-top height of 125.5 mm. While this could be reduced by optimizing the bevel gears and motor, it is unlikely that much vertical distance can be eliminated due to the fundamental design issues.

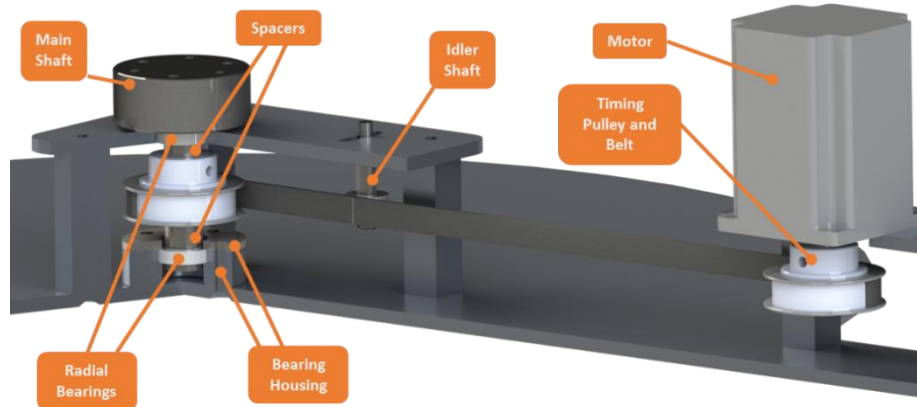


Figure 5 Section view of the belt-pulley transmission design

Figure 5 shows a similar set-up using a 1:1 timing belt-drive. Pulleys of equal size are used to transmit torque from the motor, which were orientated vertically and positioned outside of the radius of the turntable. This meant that the height of the turntable could be reduced with a base-to-top height of 99 mm. While increasing the width of the rig would make the design less compact, there was now more space available to place the electronic control components. Ultimately, the timing belt-drive setup was chosen. This was partly due to the lowered height, but mainly as the timing belt transmission gave more design flexibility, where if a change in transmission ratio was required, there would be minimal adjustments to the other transmission aspects such as shaft thickness or width. As opposed to a bevel gear, where the change in gear ratio would result in a height change of the gear and therefore repositioning of the motor, among other changes.

7.2.3 Motor Choice

A motor was required to drive the transmission system so that scans could be taken from multiple sides of the object. From preliminary research, Structured Light Scanning does not require scans to be taken at many different angles, just that the scans overlap. Since the projection and capture process is relatively quick, it was unlikely that the total scan time would exceed one hour so there was no reason to rotate the turntable too quickly. Hence, rotational speed (ω) was initially set as 4 revolutions per minute.

The motor would need to supply enough torque to overcome the load inertia I due to the turntable, 20 kg object, and main shaft. As the object may not always be placed in the centre, calculations were carried out for three scenarios:

1. Object modelled as distributed load across the entire turntable
2. Object modelled as point load acting at the centre of turntable
3. Object modelled as point load acting at the edge of the turntable

In each scenario, the inertia of the shaft and turntable is constant and only the inertia due to the object varies. Acceleration from rest to maximum speed was estimated to take five seconds t_0 and Equation 1 was used to determine the torque T for each scenario, as shown in Table 7. Friction was difficult to estimate since it would arise mainly as a result of any manufacturing errors.

$$T = I \frac{\omega}{t_0} \quad (1)$$

Table 7 Inertia and torque values for each scenario

Scenario	$I (kgm^2)$	$T (Nm)$	Load to rotor inertia
1	0.708	0.0593	14.7
2	0.083	0.0069	1.7
3	1.330	0.1120	27.8

Given that the turntable moves in steps rather than in a continuous rotation, a stepper motor was selected since the configuration process was fairly simple as opposed to using a DC motor which would require additional electronics for the same level of control. The motor has a holding torque of 1.89 Nm which is over sixteen times greater than the torque required in the worst-case scenario and was therefore likely to overcome any friction (16). Ideally, the ratio of load to rotor inertia would be less than ten (17) so that the object could be positioned more precisely but motors with higher rotor inertia exceeded the allocated budget. However, this was deemed inconsequential since the object is rotated slowly thus ensuring positional accuracy (18).

Table 8 Evaluation of a DC brushless motor and a stepper motor

Motor Type	Advantages	Disadvantages
DC Brushless Motor	Sufficient torque	Requires positional control
	Cheap	Backlash from gears
Stepper Motor	Sufficient torque	More expensive
	Rotational increments can be controlled via a motor controller	
	Load to inertia ratio less than 10:1	

7.2.4 Shaft Design

A shaft was designed for the purpose of supporting and rotating the turntable. During operation, the shaft experiences the following loads:

- Compressive axial force P due to weight of the object
- Torsion due to the torque T transmitted by the motor
- Bending moment M due to radial force R from timing belt tension while held by two bearings

A model of the shaft with the forces and moments annotated can be seen in Figure 6. Mild steel was selected at the maximum diameter offered by the Mechanical Engineering (ME) stores due to its high stiffness hence minimising deflection. A flange was included in the design to connect the shaft and the turntable together through three dowel pins and three screws. Yielding under compression was unlikely even under the maximum load of 20 kg but to avoid failure by buckling or torsion, a shaft diameter of at least 13 mm was necessary to ensure a safety factor $S.F.$ of 4.

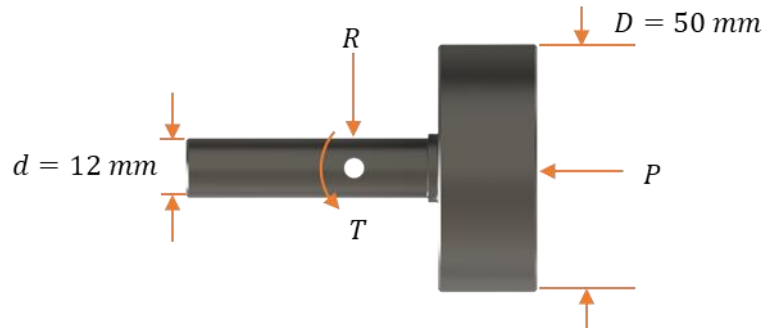


Figure 6 Mild steel turntable shaft under loaded conditions.

The belt tension F_u was calculated using the following equation from the HPC catalogue (19) where $F_{u,spec}$, Z and w correspond to the specific peripheral force, number of teeth on both pulleys and the belt width, respectively:

$$F_u = \frac{1}{2} w Z F_{u,spec} \quad (2)$$

A value of 35.3 N/cm was obtained for $F_{u,spec}$ from the HPC Catalogue (19) which, when substituted with a belt width of 10 mm and 24 teeth into Equation 2, yields a belt tension of 424 N and subsequent radial force of 847 N applied to the shaft.

By modelling part of the shaft as a beam fixed by bearings at both ends with R acting at the centre of the pulley, the maximum bending moment was found to be 6.12 Nm. Following the Von Mises criterion, the maximum stress acting on the shaft σ_{max} was then found using Equation 3, where d represents the smallest shaft diameter.

$$\sigma_{max} = \frac{4}{\pi d^3} [(8M_{max} + Rd)^2 + 48T_{max}^2]^{\frac{1}{2}} \quad (3)$$

The maximum stress was calculated to be 44.6 MPa, giving a $S.F.$ of 5.16 in relation to a yield strength of 230 MPa (20).

7.2.5 Turntable Considerations

The object to be scanned rests on and is rotated by the turntable so that scans can be taken from various perspectives to generate a complete model. From the PDS, this object can have a

maximum diameter of 500 mm and weigh up to 20 kg, so the turntable must withstand such a load whilst still being able to operate smoothly regardless of where the object is positioned on the turntable surface. Furthermore, excessive deflection of the turntable could have an effect on the stability of the object and scan quality, thus the turntable must also not be too thin. From the ME stores, aluminium sheet metal was only available in thicknesses of up to 5 mm, and as such, an aluminium disk of diameter 500 mm and thickness 5 mm was selected for preliminary analysis.

A cantilevered beam was used to model the turntable (Figure 7) where the beam's breadth b is a semi-circle and can be given as a function of x , as shown in Equation 4. A rigid shaft of 25 mm radius is attached to the centre of the turntable and simulated as a built-in end, which results in a total beam length of 225 mm.

$$b(x) = 2\sqrt{0.25^2 - (x + 0.025)^2} \quad (4)$$

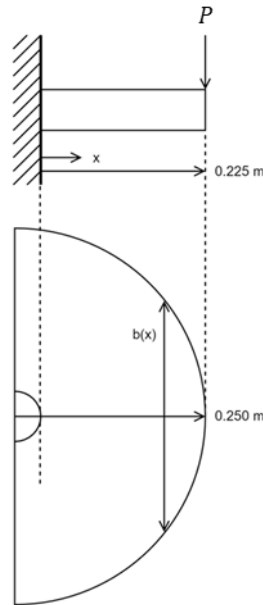


Figure 7 Turntable modelled as a cantilevered beam from side and top view.

A worst-case scenario was considered when estimating the stress and deflection wherein a point load P acts on the edge of the turntable. The bending moment profile is thus given as:

$$M(x) = 0.225P - xP \quad (5)$$

Equations 6 and 7 show the second moments of area and beam bending relations, respectively, for a rectangular cross-section where t denotes the thickness and y denotes the vertical position from the neutral axis. Substituting Equations 4 to 6 into Equation 7 provides an analytical solution for the bending stress, Equation 8.

$$I = \frac{b(x)t^3}{12} \quad (6)$$

$$\frac{\sigma}{y} = \frac{M}{I} \quad (7)$$

$$\sigma(x) = \frac{6Py}{t^3} \frac{0.225 - x}{\sqrt{0.25^2 - (x + 0.025)^2}} \quad (8)$$

Using Matlab, the stress distribution was computed from the built-in end to the edge of the turntable, shown in Figure 8 and it was clear that the maximum stress occurred at the built-in end with a value of approximately 21 MPa. Since the yield stress of aluminium is 120 MPa (21), the turntable is unlikely to yield, with a *S.F.* of 5.71 according to the Tresca criterion.

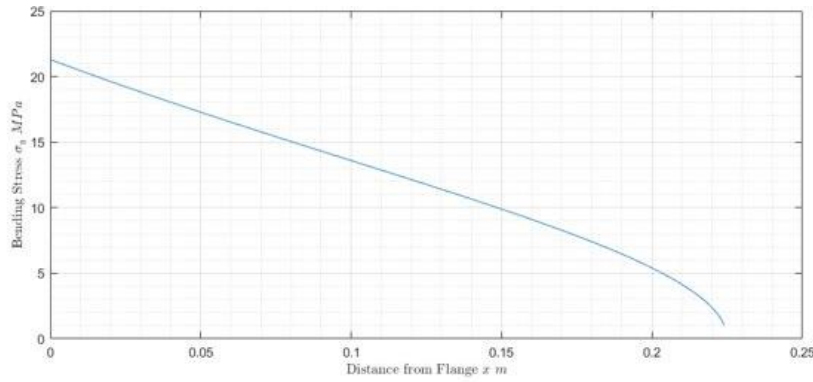


Figure 8 Radial variation of bending stress from the built-in end to the edge.

Integrating the bending moment profile shown in Equation 9 with respect to *x* provides an analytical solution for the vertical deflection *v(x)* of the turntable.

$$\frac{M}{I} = -E \frac{d^2 v(x)}{dx^2} \quad (9)$$

Figure 9 shows the variation of the deflection from the built-in end to the edge of the turntable with a maximum value of 2.2 mm. This was considered insignificant compared to the overall dimensions of the turntable so was unlikely to present any problems affecting scan quality.

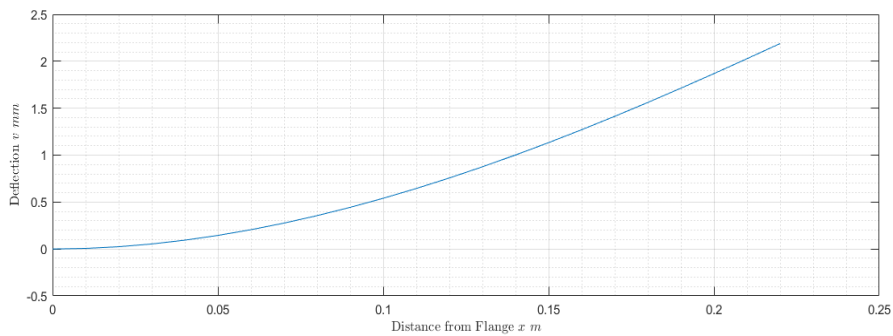


Figure 9 Deflection of turntable against distance from centre flange.

7.3 Scanner

7.3.1 Theoretical Background

Before considering the practical aspects of SLS, it is first necessary to understand the theoretical fundamentals of this project in order to inform further design decisions.

It is common in SLS to treat the camera as a pinhole model, where the aperture of a camera is assumed to become a single point known as the centre of projection. Each point or pixel on the image plane (the photograph) represents a ray going to that point, through the centre of projection, to a location on a 3D object being photographed, similar to the human eye (22).

The relationship between an arbitrary point on the 2D image plane $(u, v, 1)$ and the world coordinate (x_w, y_w, z_w) is given as (23):

$$\lambda \begin{pmatrix} u \\ v \\ 1 \end{pmatrix} = K[R, T] \begin{pmatrix} x_w \\ y_w \\ z_w \end{pmatrix} \quad (10)$$

The scalar λ represents a scale factor, while matrix R represents a 3×3 rotation matrix while vector T is a translation vector, given as:

$$[R, T] = \begin{bmatrix} r_{11} & r_{12} & r_{13} & t_1 \\ r_{21} & r_{22} & r_{23} & t_2 \\ r_{31} & r_{32} & r_{33} & t_3 \end{bmatrix} \quad (11)$$

Together, these two parameters are known as the extrinsic parameters of a camera and maps the physical location and orientation of the camera with respect to a world coordinate system.

Matrix K accounts for the differences in units between the camera coordinate system (using pixels), and the world coordinate system, as well as any inherent tilt or skew of the image.

This matrix has five unique parameters as shown below:

$$K = \begin{pmatrix} f_1 & \gamma & u_0 \\ 0 & f_2 & v_0 \\ 0 & 0 & 1 \end{pmatrix} \quad (12)$$

The two parameters f_1 and f_2 represent the focal lengths along the u and v axes of the image plane, while γ represents the skew between these two axes. The pair (u_0, v_0) are the coordinates of principal point, the intersection of the optical axis and the image plane.

Collectively, these five values are known as the intrinsic parameters of the camera and can be extended to model radial distortion from lenses.

A projector can be viewed as an inverse pinhole camera, with the light rays emerging from the image plane to the object. In the case of projection, the image plane is simply an image that one wishes to project.

It is common to include the scaling factor λ inside the term $K[R, T]$ and collectively referred to as the camera or projector matrix P_c or P_p respectively. The process of obtaining these matrices is known as calibration.

Given a certain 3D point in the global coordinate plane, the following equations describe the relations to the camera and projector image planes:

$$[u_c, v_c, 1]^T = [P_c][x_w, y_w, z_w]^T \quad (13)$$

$$[u_p, v_p, 1]^T = [P_p][x_w, y_w, z_w]^T \quad (14)$$

From the above equations, it is seen that there are three unknowns (x_w, y_w, z_w) with two equations. The last part to recovering the 3D world coordinates from the image coordinates of the projector and camera is to obtain a relationship between (u_c, v_c) and (u_p, v_p) . This process is known as encoding, whereby a one-to-one relationship between the projector and camera pixels is established.

While encoding takes different forms, the core idea is that the projector projects a known pattern which is captured on the camera and decoded based on prior knowledge of that pattern. Such a pattern can take the form of unique colours, sinusoidal gradients, or binary patterns. It is important that these patterns are unambiguous enough that a pixel on the projector cannot be misrecognised on two different areas of the photo.

7.3.2 Approach and Resources

7.3.2.1 Breakdown and Prioritization

After looking at different projects and commercial products, we divided the SLS process into four distinct stages, as shown below:



Figure 10 Workflow and processes of Structured Light Scanning.

Also shown in the above Figure 10 are the tools and software we have used throughout the SLS process. As per the PDS requirement for software or code to be accessible for future users, all resources used are open source and free to download on the internet, with links found on the project's GitHub.

Calibration and reconstruction were deemed the most important part of the process, given that the output of our product would be directly affected by the quality of resources we used.

The type of calibration and encoding method used would thus determine the nature of the image acquisition process.

7.3.2.2 Calibration and Reconstruction

The bulk of the two aforementioned processes is done via Taubin and Moreno's Scan3D software. This was chosen specifically for their calibration method, which involves simultaneous calibration of the projector and camera via Zhang and Huang's (24) method, which has the advantage of calibration speed and reducing calibration errors. Traditionally, the calibrated camera is then used to calibrate the projector, which causes propagation of errors or uncertainties. An accurate calibration process is especially important as this affects the quality of the reconstructed mesh, as shown by Taubin and Moreno (25).

7.3.2.3 Post Reconstruction Treatment

As SLS takes the depth profile of the object facing the projector, there is a need to capture the same object multiple times in different orientations to get complete 3D information. This implies that multiple views must be oriented and stitched together, which can introduce significant errors if done visually by hand.

Once reconstructed point clouds from multiple views have been obtained, we decided to use CloudCompare and Meshlab, both open source software, to handle the alignment of point clouds and mesh generation, respectively. CloudCompare was chosen due to its intuitive interface and use of the Iterative Closest Point (ICP) algorithm to minimise the errors in alignment, while Meshlab for the customisability in mesh reconstruction to suit different surface textures and irregular geometry.

7.3.2.4 Image Acquisition

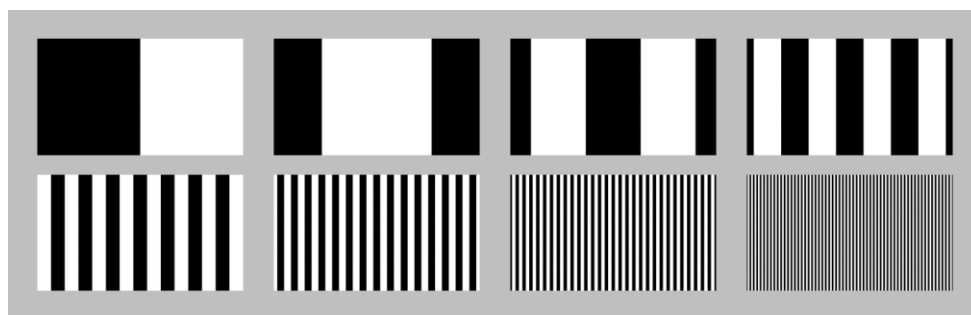
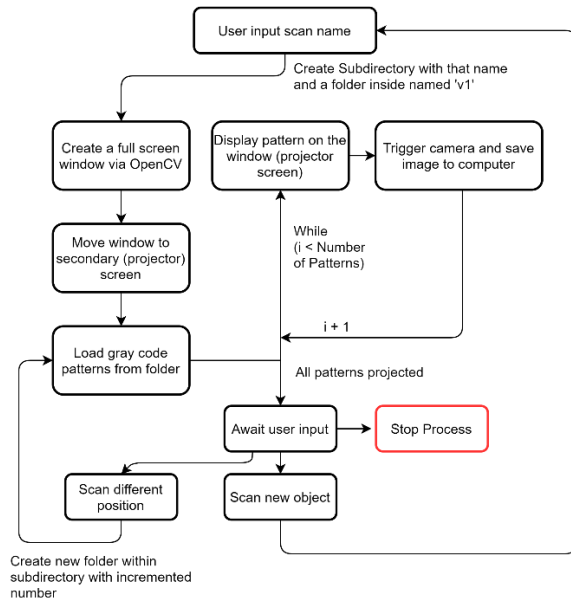


Figure 11 Series of patterns that constitute grey code temporal encoding.

Scan3D uses grey code temporal encoding, where a sequence of black and white images such as those in Figure 11 are projected and captured by the camera per view of the object. As such, image acquisition requires the generation of these grey code patterns in the appropriate

resolution of the projector. This was done using Matlab, although Python's OpenCV module also has the same functionality.



In order to project a sequence of images and automatically take images, the projector is treated as a second screen, and the Python package OpenCV is used to display these patterns to be projected. A simplified workflow is shown in Figure 12.

The actual trigger mechanism for photo taking is dependent on the type of camera used and will be discussed in greater detail in Section 8.

Figure 12 Workflow of Image Acquisition Script.

7.3.3 Scan Components

In order to implement SLS, a minimum of one projector and one camera is needed. Given a budget constraint of £1000, we had originally aimed to spend up to £400 on these two components, with the intent that the equipment could be used for both the initial prototype and the final design. Table 9 lists the main factors affecting our choice of projector and camera:

Table 9 Summary of scanning hardware selection criteria.

Factor	Component	Description
Resolution	Projector and Camera	A higher camera and projector resolution would increase the points encoded for the same area, thus increasing point cloud density.
Throw Distance	Projector	This is the distance from the projector lens to the screen surface for which the image is sharp, usually given as a range. A shorter throw distance is desirable as the overall product would be more compact.
Screen Size	Projector	The larger the percentage the scanned object occupies, the more points can be encoded to describe it. As such, a screen size as small as possible is desirable, yet still able to capture the whole object.
Shutter Control	Camera	As image acquisition is automated, the camera must be able to support remote triggering.

From the factors above, it becomes apparent that a suitable projector must have a screen size of at least 500x300 mm, the dimensions of the largest object to be scanned, while having a short throw distance. Manufacturers often also specify the throw ratio, a constant which links the two properties, given by:

$$\text{Throw Ratio} = \frac{\text{Throw Distance}}{\text{Image Width}} \quad (15)$$

Decreasing the throw distance would thus decrease the projected image size, which is desirable up till the minimum width and height limit. With these considerations in mind, the AAXA P300 Neo Projector was selected with a resolution of 1280x720.

This projector has a throw distance range of 508 – 2032 mm and projected image dimensions of 376x212 mm at minimum throw distance. From the above equation, the projector should be at least 720 mm away from the object for a screen size of 533.3x300 mm, to scan an object of maximum width, thus achieving a good compromise.

The Logitech C920 webcam was selected based on hardware recommendations by other structured light projects (26) (27). Additionally, this webcam has interfacing functionality with Matlab (28), thus is able to be controlled remotely via a script. This camera has a resolution of 1920x1080 and should be able to capture the grey code patterns as it has a higher resolution than the projector.

7.4 Control

Given that the object must be rotated in increments and is stationary while being scanned, a successful control system must ensure that:

- The turntable must move a set angular distance smoothly and reliably within a reasonable margin of error
- The effect of loading should not significantly influence the angular distance moved and the angular velocity during operation
- The overshoot, if any, and settling time should not be excessive

As a prototype, it is necessary to investigate these parameters of the system, in order to make informed design decisions during further iteration. Two dominant control methods are considered, direct open loop control and positional feedback control, shown in Table 10.

Table 10 Evaluation of direct and feedback control.

Control Type	Advantages	Disadvantages
Direct Control	Simplicity of design with minimal electrical components	Cannot minimise the error from an external disturbance No direct control over steady state error or transient behaviour
Feedback Control	In tandem with a Proportional Integral Derivative (PID) controller, can fine tune both the steady state error and transient behaviour Can respond to unexpected disturbances	Requires knowledge of turntable position via sensors, complicating the electrical setup

The method of direct control was chosen, as simplicity of design was valued over the potential benefits of error and transient control. This was as primarily because feedback control was possible to implement on top of the existing direct control setup, and thus if prototype testing

results were unsatisfactory, the alternative control method could be built upon what was existing.

Furthermore, the scanning demands do not require knowledge of the absolute angular position, but rather the relative change between each turn, as the alignment process does not need any prior rotation or translation estimate. Also, as a stepper motor is used, a fairly accurate turn angle can be specified as long as the torque involved in deceleration does not exceed the motor holding torque. Lastly, a turntable setup is unlikely to experience any external disturbances, given both the operating environment and the constant weight of the object on the turntable, and would not need to account for that factor.

For rapid prototyping, the Arduino Uno was used to send commands to the motor. A stepper motor driver is also needed to interface with the stepper motor, and the Pololu A4988 Driver Carrier (29) was selected, with micro step resolution of up to one-sixteenth allowing for smoother movement.

8 Prototype Testing

A series of tests were carried out to assess the scanning system against the requirements in the PDS and to evaluate the system's performance and operations. The scanning system consists of two critical elements, the scanning device which is comprised of the camera and the projector, and the turntable. The prototype testing was targeted at these two components and relevant tests were done according to the established criteria for each component.

Once both systems were tested for their individual functionality, they can then be integrated into a homogeneous system, with findings used to improve and inform aspects of the product.

8.1 Turntable

To test the operation criterion, it was subjected to mechanical and electrical tests. These tests were carried out in the Dynamics lab, which offered an assortment of testing instruments, equipment, technical guidance, and a worktable, making it a suitable location for most of the testing to take place. The subsequent sections detail the various tests' aims, procedures and results.

8.1.1 Structural Integrity Test

Aims of Test:

1. Assess the structural integrity of the turntable system by confirming if the actual deflection measurements of the turntable are the same or less than the calculated deflections.
2. Assess how the turntable deflection is affected by varying the loading position radially across the turntable

Testing Context:

The turntable must support a maximum load of 20 kg regardless of eccentric or non-eccentric loading. As a result, the turntable, shaft, and other connected components must not exhibit plastic deformation which may lead to structural failure. Analytical and numerical methods such as Macaulay's method and Finite Element Analysis were calculated prior to testing to obtain a rough estimate of what experimental values for deflection should be obtained.

8.1.1.1 Testing Methodology

A dial gauge was used to determine the end deflection caused by loading. The dial gauge was placed near the edge of the table as shown in Figure 13 and was subsequently zeroed. The deflection was then read from the dial gauge.

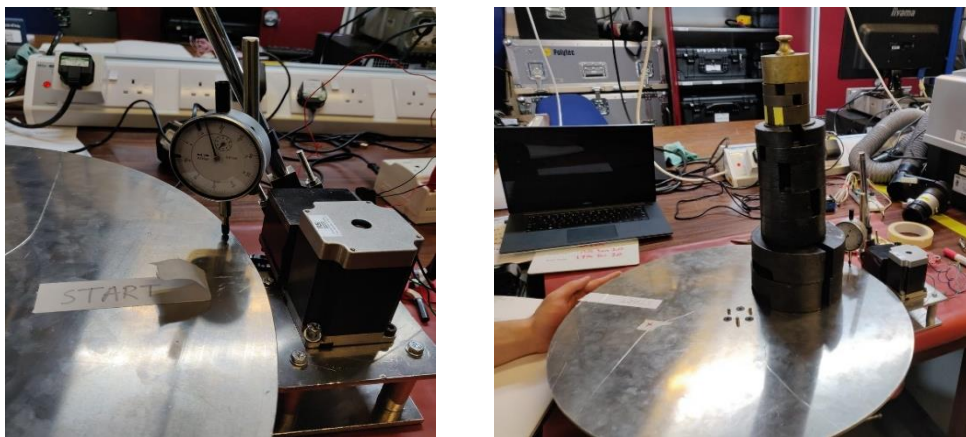


Figure 13 Experimental set-up using a dial gauge to measure turntable deflection

Combinations of known weights of 10, 20, 50, and 100 N were loaded 125 mm from the centre of the turntable, as shown in Figure 13. The distance was measured from the turntable centre to the geometric centre of the weights, where the geometric centre is assumed to be the centre of mass of the weights. The radial distance of 125 mm was chosen as it was the furthest the weights could be set without extending past the turntable. Weights were added in increments, up to 200 N and the reading on the dial gauge is recorded after each increment. The experiment was repeated with the weights placed on the diametrically opposing side of the turntable so that the deflections from another similar point of loading can be obtained. This was to reduce the possible influence of manufacturing defects on the test results.

8.1.1.2 Analytical Method

Similar to the analysis in Section 7.2.4, the turntable is modelled as a cantilevered beam, but this time with the force at 100 mm away from the built-in end instead to match conditions of the experiment.

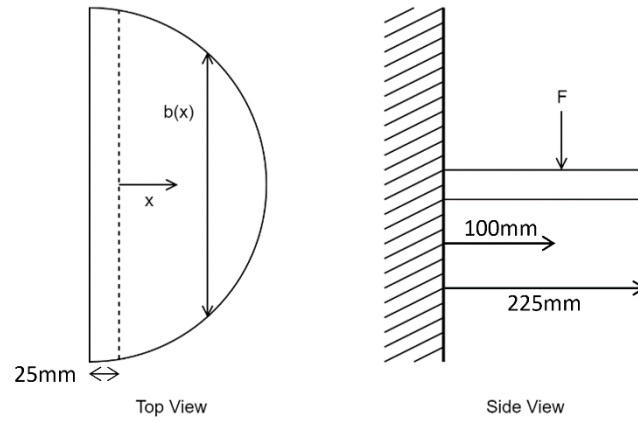


Figure 14: Turntable modelled as a cantilever

The new bending moment profile is thus:

$$\begin{aligned} 0 < x < 0.1 : M(x) &= 0.1F - xF \\ x > 0.1 : M(x) &= 0 \end{aligned} \quad (16)$$

Similarly to before, the analytical deflection was computed and the end deflection recorded for each load that was placed on during the experiment.

8.1.1.3 Finite Element Method

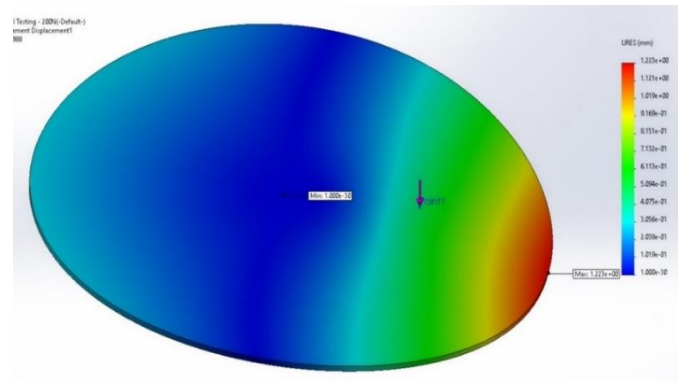


Figure 15 FEA analysis of turntable

An aluminium plate of diameter 500 mm was used to model the turntable. A fixed boundary condition was imposed over a circle diameter of 50 mm around the centre of the underside of the model. This is to simulate a rigid shaft that is affixed to the centre of the turntable. A point load of was imposed 125 mm away from the centre of the model. An H-adaptive mesh with a maximum of 3 iterations was used to refine the mesh, before running the simulation. FEA was performed on the model with incrementing loads up to 200 N, with the end deflections recorded for each load. Figure 15 shows the deflection profile of the plate where the point load is 200 N, showing maximum deflection at the plate end, similar to the analytical graph obtained prior.

8.1.1.4 Test Results and Observations

The graph of deflection against weight is plotted in Figure 16 below:

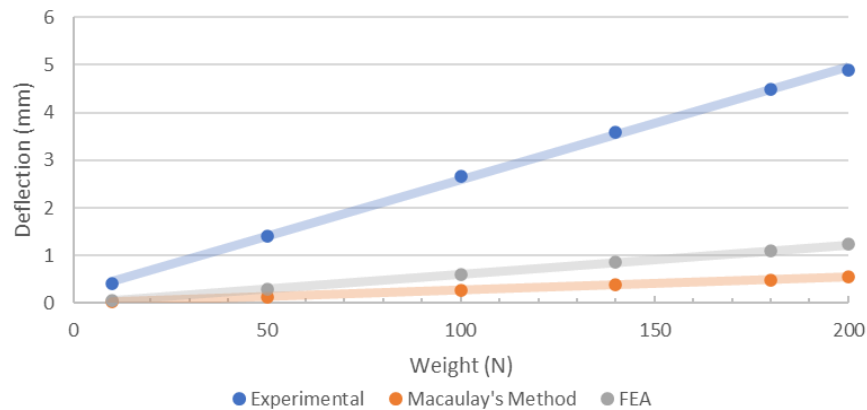


Figure 16 Comparison of experimental deflection results to FEA and Macaulay's method

At 200 N, the empirical results yield a much higher deflection of 4.90 mm than the other two benchmarks, with the FEA analysis giving 1.23 mm and the analytical method giving 0.55 mm. This is also observed across the different weights. The greater empirical deflection can be attributed to several reasons such as the inaccurate assumption of the shaft being completely rigid and acting as a built-end in the analytical method and FEA, or leeway due to inexact tolerances in the shaft, gears, or bearings. Furthermore, it was found out that the shaft was machined out of aluminium instead of steel due to a miscommunication error. This could contribute to additional tilting of the plate as the less stiff aluminium shaft would bend more than steel.

Out of the aforementioned reasons, leeway from inexact tolerancing, not bending, is likely to have a large influence on the large deflection values. Therefore, the difference between the lowest experimental deflection values at 10 N and subsequent deflection values would give a more accurate actual deflection value. It is probable that the FEA results give a better estimate of the 'true' plate deflection, as the assumption of constant deflection at any cross section in the analytical model is unlikely to hold.

It was also noted that there was no plastic deformation of the turntable in the experiment as the dial gauge reading returned to zero when the turntable was completely unloaded. No yield in the turntable also indicates that the turntable is unlikely to fail unexpectedly under these loading conditions.

8.1.2 Electrical Controls Test

Aims of Test:

1. Determine the viability and effectiveness of the stepper motor and the Polulu A4988 motor driver working in tandem with the Arduino Uno
2. Determine the effective micro stepping settings for smooth movement
3. Determine if the turntable will operate and rotate to the required angle of 90° when the turntable is loaded up to 20 kg regardless of the loading position on the turntable
4. Investigate the rotation time and settling time of one rotation with respect to the loading of the turntable

Testing Context:

The angle of rotation of the turntable must be able to be controlled for an optimal number of scans to be taken of an object. The optimal number of scans is dependent on the object's size and geometry, with large irregularly shaped objects requiring more scans, and hence finer rotational control.

8.1.2.1 Stepper Motor and Arduino Configurations

Before the start of the test, the optimal motor settings such as the need for micro stepping and the delay between steps for the stepper motor have to be resolved as they respectively affect the smoothness of operation and speed of rotation. Micro stepping is when a stepper motor is rotated at a fraction of a step, usually one eighth or one sixteenth of a full step. The motor driver was initially configured to have full steps and the number micro steps was subsequently increased until the turntable was observed to run smoothly.

At a micro step of one sixteenth, the turntable did not exhibit jerky behaviour. It was also found that a delay of 40 milliseconds between steps resulted in the turntable taking approximately 11 seconds to complete a 90° rotation.

Since the stepper motor normally has a step size of 200 steps per revolution, a sixteenth step configuration would give a modified step size of 3200 steps per revolution. The Arduino was then programmed to rotate the turntable to a 90° angle with the press of a button, with a total step number of 800.

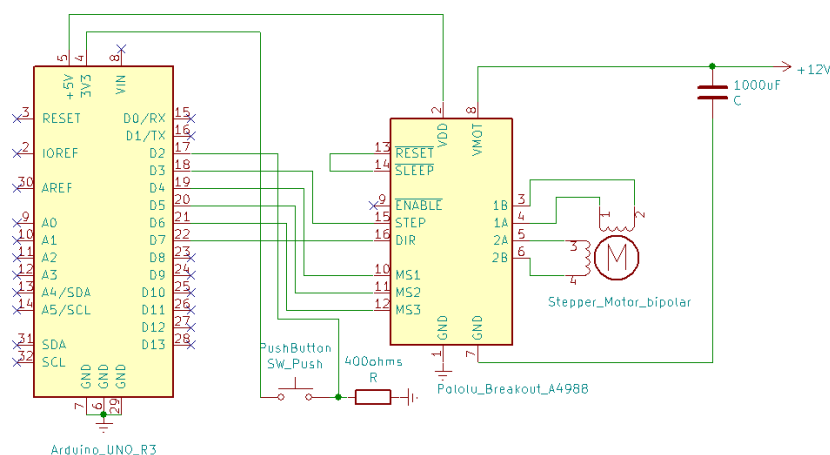


Figure 17 Schematic of the integrated electrical controls system

Figure 17 shows the electrical schematic of the setup. The Arduino Uno was powered via Universal Serial Bus (USB) by a computer, while a 12 V power supply powered the motor driver and thus the motor. The three inputs MS1, MS2, and MS3 allow configuration of micro-stepping settings.

8.1.2.2 Testing Methodology

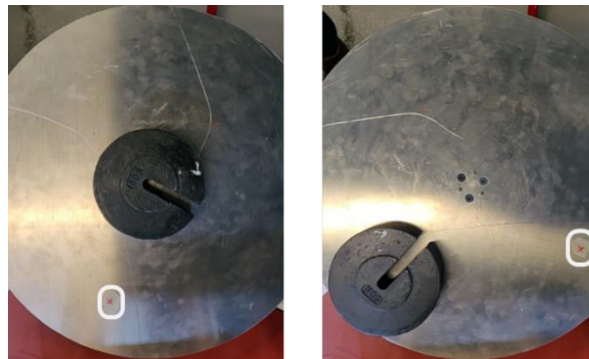


Figure 18 Experimental setup for tracking angular position

For the test, a marker was placed near the edge of the turntable and the video recording device, a smartphone, is set up to record the top-down view of the turntable, shown in Figure 18 above. Similar to the structural integrity test, the weights were placed either at the centre or at 125 mm away.

The turntable was initially unloaded and with the press of the button, rotated 90° . The turntable was subsequently loaded at the centre of the turntable in 50 N increments up till 200 N. After each increment, the turntable rotated 90° and the weights were added only after the turntable had come to a complete stop. Four turns were recorded for each weight increment in order to determine if the absolute angular position affected any turning behaviour. This process was then repeated for the eccentric loading to simulate the worst-case loading scenario.

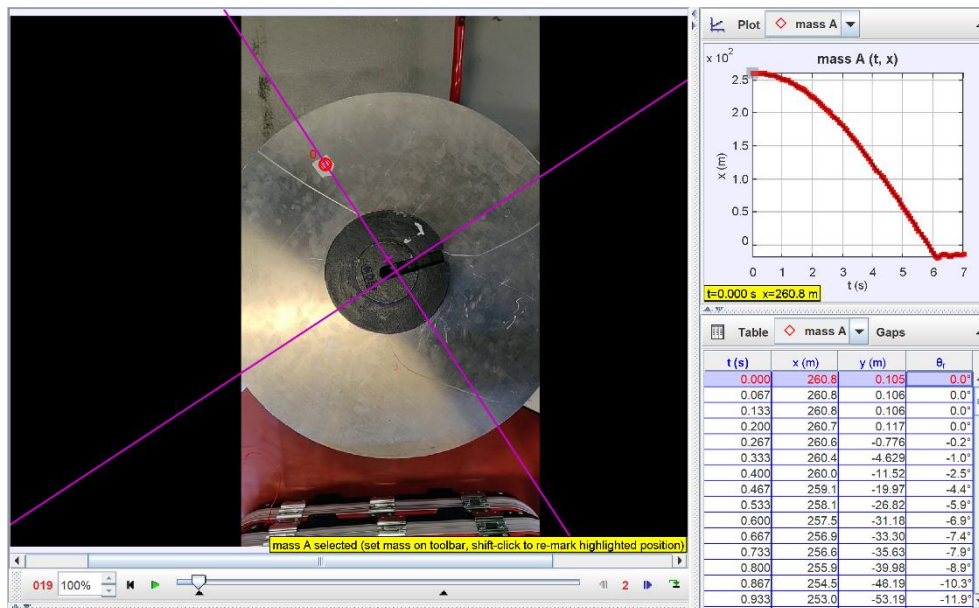


Figure 19 Tracker software interface

The video recording was then edited into individual clips of rotation at each weight and the clips were uploaded into a program called Tracker, which tracks the position of the marker throughout the turntable's rotation. A reference coordinate system was set initially to align with the marker as shown in Figure 19. As the turntable rotates, the software tracks the marker and records its coordinates relative to the coordinate system, stored as seen from the bottom right of Figure 19. The angle of rotation and scan time were also obtained from the software. From the data provided, the time taken for the rotational angle to settle to 90° from start was recorded as the total scan time. The settling time is calculated by deducting rise time from the total scan time, where the rise time is the time from start till the greatest rotational angle was reached.

8.1.2.3 Test Results and Observations

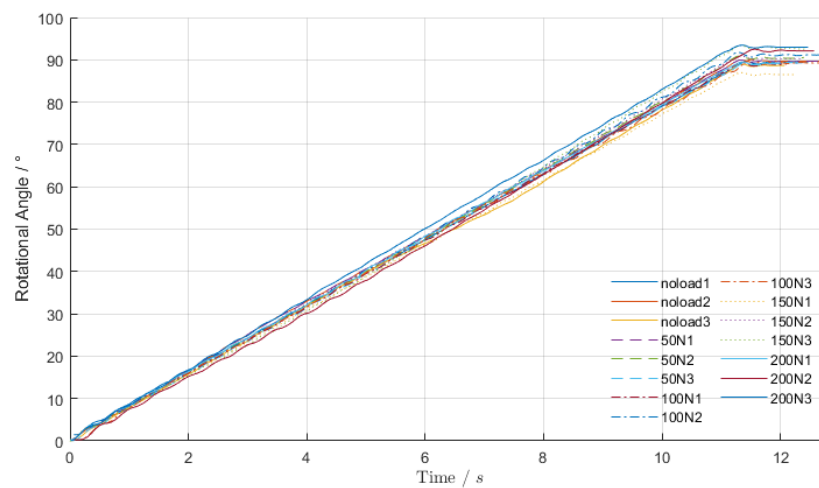


Figure 20 Graph of rotational angle against time when centrally loaded.

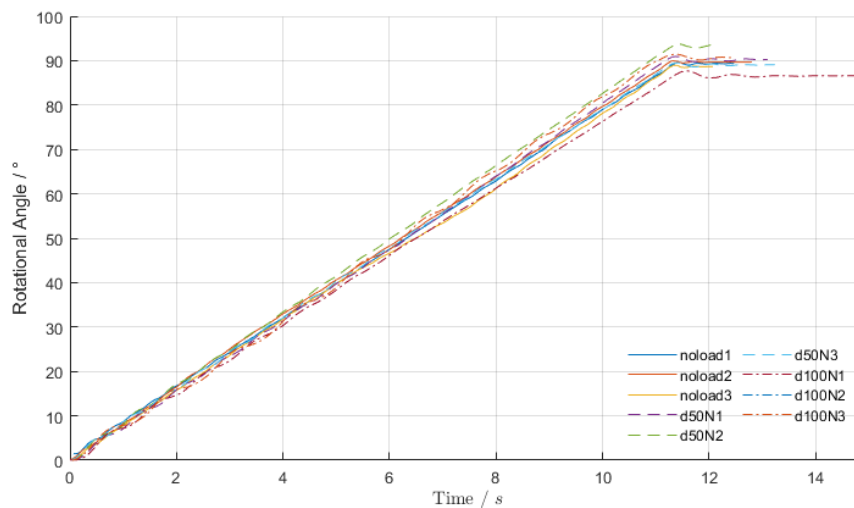


Figure 21 Graph of rotational angle against time when eccentrically loaded.

Table 11 Averaged results of the Electrical test.

Position of mass	Weight (N)	Rotational Angle (°)	Total time (s)	Settling time (s)
Centre	0	90.5	10.94	1.92
	50	89.8	11.09	2.01
	100	89.8	11.12	2.03
	150	89.8	10.97	1.99
	200	91.4	11.07	2.05
Off-centre	50	90.9	11.04	2.00
	100	89.3	10.94	2.16

The graphs for angular displacement against time for both the centrally and eccentrically loaded turntable is shown in Figures 20 and 21, with the averaged results, total time, and settling time shown in Table 11 above.

It was noted that when the turntable was loaded eccentrically with 150 N weight, the turntable could not rotate reliably and thus, data for more than 100 N could not be obtained in this test. Possible explanations for why this occurred will be discussed in Section 9.

A comparison of rotational angle across the different loading conditions shows that the turntable can rotate to a predefined angle consistently as all the values obtained were approximately within 1° of the desired 90° which is approximately an error of 1.1%.

The time taken for the rotations can also be seen to be independent of the loading conditions and has an average of 11.02 seconds. Similarly, the settling time appears to remain approximately constant throughout the different loading conditions.

8.2 Scanner

Aims of Test:

1. Obtain data on physical requirements to guide the mechanical design process
2. Identify pitfalls and best practices to refine the scanning process
3. Carry out a scan on a simple object as a proof-of-concept ensuring that the resources used, and the code written can produce a 3D model of that object

Testing Context:

As scanner design would significantly influence mechanical design, an early preliminary test was essential to determine whether Structured Light Scanning could produce a 3D model given the available resources. Therefore, it was important to front-load the Structured Light Scanning proof-of-concept in the design process to reduce the risk of having to redesign the entire system later.

As mechanical engineers, the theories and processes of Structured Light Scanning have not been previously learnt, and a better understanding of the SLS process would be required in order to make more informed choices on the physical aspect of the product.

Multiple tests were conducted throughout the academic year, with findings from each test improving the subsequent tests. The following section describes the general methodology to obtain scan data and the subsequent section will describe the differences between tests.

8.2.1 Testing Methodology

8.2.1.1 Set-Up

The camera and projector are placed about 300 mm apart, and the location where the object will be placed is marked. The projector is adjusted such that the projected images lying on the object are mostly within focus and sharp, while the whole projected screen must fit within the boundaries of the captured image.

8.2.1.2 Calibration

The image acquisition process has two stages, one for calibration of the projector and camera, and the other to obtain data of the image. In order to calibrate the projector and camera, a printed black and white checkerboard pattern on a rigid backing is needed. For purposes of the test, this pattern is printed and attached to a piece of cardboard, shown in Figure 22. During the process, the relevant parameters to be taken note of are:



Figure 22 Checkerboard pattern on calibration board.

- Number of internal corners of the pattern. In Figure 22 above, there are 8 corners horizontally and 10 corners vertically
- Dimensions of each individual square in millimetres

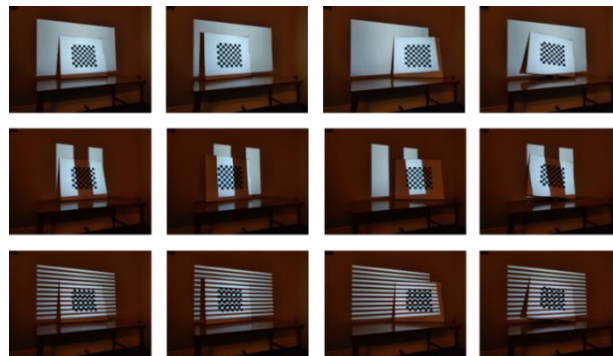


Figure 23 SLS calibration process.

This calibration panel is then placed in front of the screen at the marked spot, and the grey code patterns will be projected sequentially. The camera will then capture each pattern, saving the images as one set. The panel is then moved to a different position and the process is repeated, as illustrated in the Figure 23 above. The calibration software requires a minimum of three unique positions with the entire panel remaining within the projected screen.

8.2.1.3 Scanning

The actual scanning process is similar to that of calibration, where the object to be scanned is placed at the marked spot, and the same grey code patterns projected sequentially and captured. After all images have been projected and captured, the depth profile of the side of the object facing the projector can then be recovered.

It is important to note that once the camera and projector have been calibrated, any movement of these two devices relative to each other will render the prior calibration invalid, and an inaccurate depth profile will be reconstructed.

8.2.1.4 Automation

As previously mentioned in Section 7.3.2, the image acquisition process was automated such that pictures are taken in sync with the projection of images, with each set of images being stored in individual folders. The need for remote trigger control was an integral part of automation, yet different cameras use different methods of interfacing with a computer. As such, multiple scripts of the same process were written but with different image capturing devices in mind in Table 12:

Table 12 Summary of trigger control methods for various camera devices.

Device	Trigger Control Method
Webcam	Use of Python's computer vision module cv2 to obtain a live video feed and save a snapshot of that feed in sync with projection.
Digital Single Lens Reflex (DSLR) Camera	Use of the gPhoto2 (30) open source application for Unix-like systems, controlled by console commands. This is integrated with Python using the subprocess wrapper <i>sh</i> (31).
Android Phone	The free application IP webcam (32) is installed on the phone, which has a web interface for remote control. This is integrated with Python using the URL interfacing module <i>urllib.request</i> (33) to allow automatic remote trigger control.

Remote trigger for the webcam was written in mind for the Logitech C920 webcam intended for actual use in the product, while trigger control for a phone was written for automated image capture before the webcam was ordered. DSLR trigger control was written with future modularity in mind, as higher resolution cameras are often of that type and would require a method for automatic control.

8.2.2 Test Results and Observations

8.2.2.1 First Proof-of-Concept Test

This scan was done early in the academic year, and thus the ordered scan components in Section 7.3.3 had not arrived yet. As such, an alternate projector and camera was used. Both calibration and scanning were done with no sources of light present other than the projector.

- **Camera:** Android phone, OnePlus 6T with resolution of 4608x3456
- **Projector:** [Dr. Q HI-04](#), resolution of 1280x786, throw distance of 1.5 – 5 meters and screen diagonal size of 813 – 4470 mm



Figure 24 Wooden toy car used as the scanned object.

A wooden toy car, in Figure 24, was chosen as the model to be scanned because the object had a relatively simple geometry and was unreflective. It was postulated that a reflective surface could obscure the grey code patterns and result in an incomplete encoding.

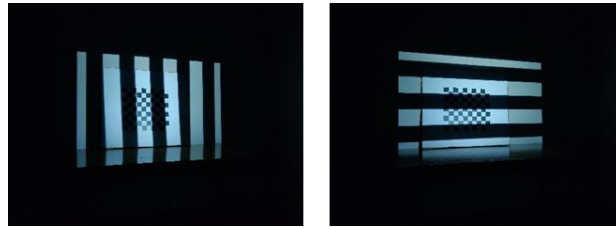


Figure 25 Manual image acquisition.

For the first test, the image acquisition process was not automated, with pictures shown in Figure 25 as a slideshow on the projector and the camera phone operated manually.

Unfortunately, the algorithm was unable to detect the corners of the calibration panel from the images taken. This was attributed to the images being too dark, whereby the checkerboard patterns could not be visible in the 'off' patterns of the grey code.

8.2.2.2 Second Proof-of-Concept Test

In this test, the setup was similar to the previous, but with the presence of ambient lighting, such that the checkerboard can be seen in the darker portions of the pattern. The same toy car model was used. The primary aim of this test is to determine if the ambient lighting conditions was responsible for the failure in the previous test.

```
% Projector-Camera Stereo calibration parameters:

% Intrinsic parameters of camera:
fc_left = [ 3449.572679 3415.736572 ]; % Focal Length
cc_left = [ 2433.465076 1751.492272 ]; % Principal point
alpha_c_left = [ 0.000000 ]; % Skew
kc_left = [ 0.294919 -2.271333 -0.001734 0.020312 0.000000 ]; % Distortion

% Intrinsic parameters of projector:
fc_right = [ 1041.530849 2039.755642 ]; % Focal Length
cc_right = [ 494.745665 620.753046 ]; % Principal point
alpha_c_right = [ 0.000000 ]; % Skew
kc_right = [ 0.079825 -0.591723 -0.002904 0.000495 0.000000 ]; % Distortion

% Extrinsic parameters (position of projector wrt camera):
cm = [ 0.019425 0.455165 0.025732 ]; % Rotation vector
T = [ -368.505799 -17.935244 302.050537 ]; % Translation vector
```


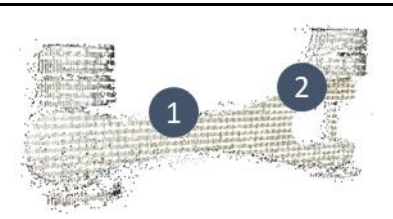
Figure 26 Screenshot of projector-camera calibration code.

The successful detection of the calibration panel confirmed the requirement for the checkerboard to be visible in all lighting conditions, and calibration parameters obtained can be seen in the Figure 26 above. Only the projector's extrinsic matrix $[R, T]$ was given, as the origin of the world coordinate was set to be the origin of the camera coordinate. Also, the rotation matrix was converted to the corresponding vector via Rodrigues formula (34).

A Python script was used to automate the image acquisition process and capturing and saving of 44 unique grey code patterns took an average of 90 seconds. The majority of this time was spent downloading the images, which were at least 3 megabytes each, to the computer.

Table 13 shows the recovered point cloud, along with some general observations:

Table 13 Observations of point cloud data.

	<ol style="list-style-type: none"> 1. Due to projection screen size, the toy car takes up only a small proportion of the screen, resulting in fewer pixels being able to describe the model. 2. General warping of the background wall near the edges, implying that the calibration parameters might not be valid at the fringes of the screen. 3. A lot of erratically spaced points, especially at the base of the wall, perhaps due to reflection from the smooth bench.
<p><i>Figure 27 Point cloud of toy car and background</i></p>	
	<ol style="list-style-type: none"> 1. Points in a grid-like pattern, perhaps due to poor projector resolution. This can cause 'bleed' of the columns and rows at thinner grey code patterns, resulting in an inability to properly decode the pictures. 2. Despite the poor resolution, main features such as the rear axle or the separation of the wheels can be distinguished.
<p><i>Figure 28 Point cloud of toy car only</i></p>	

8.2.2.3 Hardware Functionality Test

This test was carried out with the ordered scan components, with the specifications below:

- **Projector:** AAXA P300 Neo Projector, 1280x720p, rechargeable 2000 mAh Li-ion battery, 381 grams, 14x8.9x3 cm.
- **Camera:** Logitech C920 Webcam, 15 MP 1080p, 200 grams, 2.4x9.4x2.9 cm.

The main objectives of this test were to ensure that the webcam could be controlled remotely, and if the improvement in projector screen size and resolution would lead to a denser point cloud file.

As the throw distance of the projector is shorter than previously, the new setup consists of the webcam and projector spaced approximately 100 mm apart, and the object and calibration panel placed about 600 mm away from the projector. Ambient lighting was introduced in the form of a desk lamp above the setup.

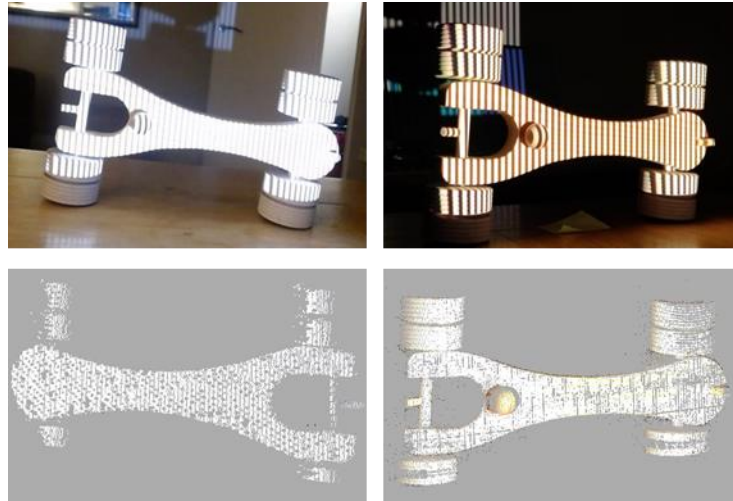


Figure 29 Comparison of point cloud files with and without exposure control.

While the webcam was controllable via a script, a major issue found was the lack of exposure and focus control. This resulted in the columns or rows of light ‘bleeding’ over to the adjacent darker columns, hampering the encoding process. The top two pictures in Figure 29 above shows the comparison of the same pattern captured using the webcam on the left and a phone (with exposure and focus control) on the right, with the resultant point clouds shown below. The point cloud density of the overexposed image is lower than the one taken with proper exposure. Even so, the point clouds for both the webcam and phone are denser than that in the second test, emphasizing the importance of projector choice.

While ambient lighting conditions can be controlled, the main source of light was due to the projector itself, thus the webcam was deemed unsuitable for SLS due to its inability to regulate focus and exposure.

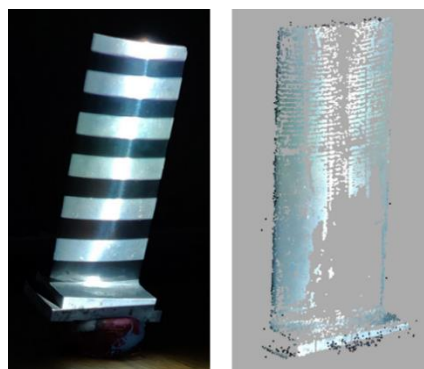


Figure 30 Point cloud of a reflective turbine blade.

In addition, a turbine blade of an engine part was scanned to investigate the effect of shiny surfaces on scan quality. In the Figure 30 above that the vertical axis of the blade strongly reflects light, and the corresponding middle section of the blade is missing on the point cloud.

It can thus be inferred that areas of high reflectivity pose an issue to the encoding and decoding process.

8.2.2.4 First Alignment and Meshing Test

This test was carried out using the AAXA P300 Neo Projector and the OnePlus 6T android phone, as prior tests have shown that the Logitech C920 webcam had issues with overexposure. In this test, the main objective was to scan multiple views of the same object, with the intention to determine any preferred practices in aligning and meshing multiple point clouds into a complete 3D model.

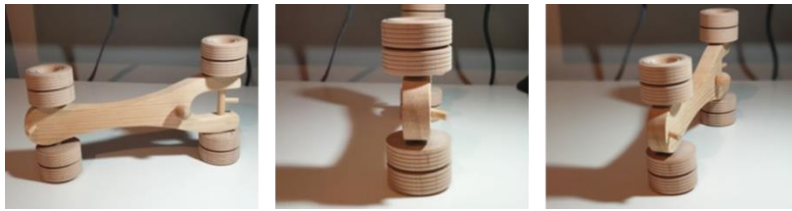


Figure 31 Front and side views of wooden toy car.

Similar to the previous test, the toy car was used as a model, and 10 views were taken at different angles, with some shown in the above Figure.

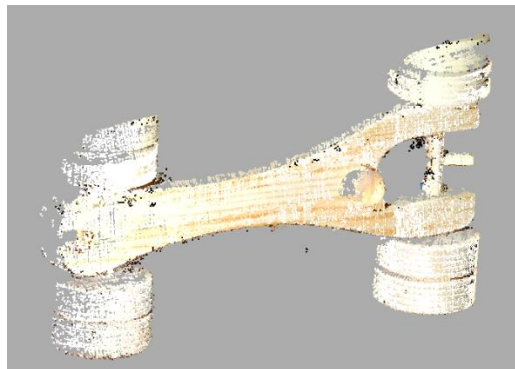


Figure 32 Aligned point cloud stitched together from different scans.

However, issues arose during alignment, as sharp angles such as transitioning from a frontal view to a side view, from the first picture to the second in Figure 32, caused a lack of common points between the point clouds for proper alignment to take place. As such, only a partially reconstructed model comprising of the frontal faces could be made, shown in the Figure above.

8.2.2.5 Second Alignment and Meshing Test



Figure 33 Cardboard Amazon delivery box to be scanned.

A final test was conducted, with the goal to successfully construct and mesh an object. While the scanning setup and conditions were kept constant from the previous test, a cardboard box, shown in the Figure 33 above, was chosen instead. This was because a non-reflective, geometrically simple object with clearly recognizable features was preferred to allow easy alignment. The regular geometry also ensured no sharp corners or angles, and thus would theoretically require fewer unique views to get a full model.

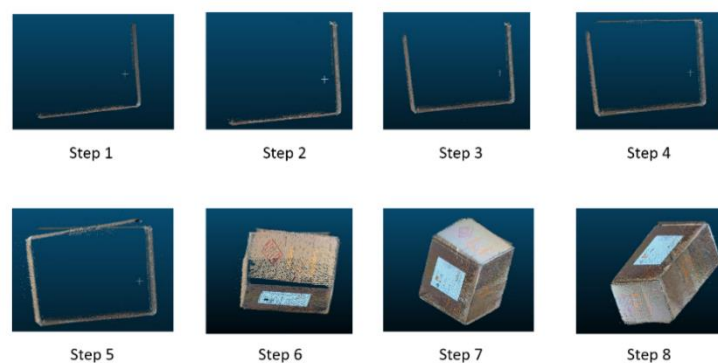
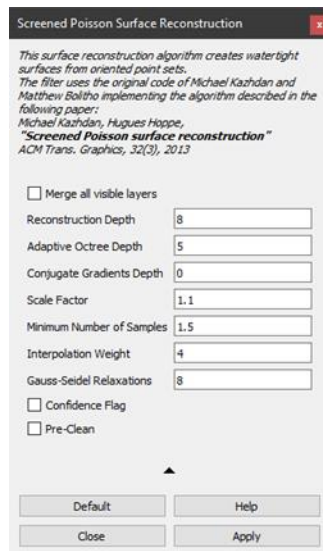


Figure 34 Point cloud aligning process for cardboard Amazon box.

A total of 18 views were taken, and Figure 34 above shows how 8 views were needed to construct a full model. It is important to note that at stage 5, the sides of the boxes are not completely parallel, resulting in an inaccurate alignment. This is caused primarily due to the warping of the point cloud for one of the views, resulting in a not completely perpendicular side. As other point clouds appeared to have no warping, this was attributed to some displacement of the scanning equipment during the scan, which was plausible given that the camera and projector were merely resting on a flat surface.



Reconstruction Depth - Meshlab

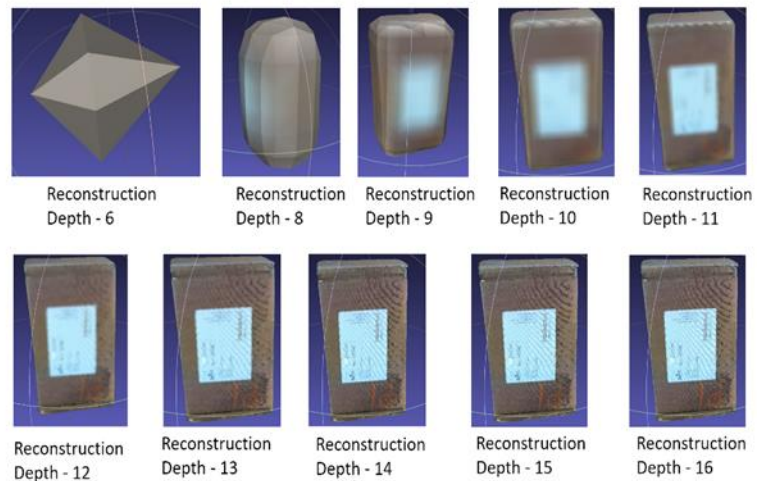


Figure 35 Generation of watertight mesh in Meshlab.

After a complete point cloud was made, a mesh was created using MeshLab. The Screened Poisson Surface Reconstruction method (35) was deemed the most appropriate to construct a watertight mesh, and the reconstruction depth, shown in Figure 35 above, was seen to have the greatest impact on the detail of the scan. It is seen that for a depth of 14 and above, there is only a marginal improvement in mesh quality, while meshing time increases exponentially.

9 Evaluation of Prototype

9.1 Summary of Prototype Tests Results

The combined results of the mechanical, electrical control, and scanning prototype tests are summarised in Table 14.

Table 14 Summary of prototype test results.

Aspect	PDS Requirements	Test Results	Achieved
Scan Volume	Support objects up to 20kg in mass	No yielding from a 20kg weight, but unable to rotate eccentrically loaded weights greater than 10kg.	No
Scanning Software	Accessible and modifiable without any prior purchase	Open-source software used. Python and Arduino scripts available on GitHub.	Yes
Scanner Output	Data must be taken from the object from all angles and preferably stored in a suitable 3D modelling format	Data taken from object from all angles and stored .ply and .stl files .	Yes
Scan Time	Total scan time to take less than 1 hour	Less than 2 minutes per scan, thus able to complete at least 30 scans per hour.	Yes

9.2 Evaluation of Structural Integrity Test

The main findings from the structural integrity test are summarised in Table 15:

Table 15 Summary of findings from structural integrity test.

Design Aspect	Findings
Turntable Strength	Can support a static load of up to 20kg when loaded eccentrically
Deformation	No permanent deformation observed, loading is within the elastic regime for all loads
Deflection	Maximum deflection of 4.9 mm at the turntable edge when loaded with a 200 N weight, exceeding the FEA-calculated deflection by four times

Although deflection was greater than that predicted by the analytical methods, there was no plastic deformation during the test and hence, the turntable will not fail when it is loaded by a 20 kg object. It should also be noted that the deflection experienced by the system will not affect the scan quality as the deflection will only result in the object being captured at a tilted angle, which will be rectified during the alignment phase in CloudCompare. However, the unexpected deflection should still be corrected as it may have unpredictable repercussions such as generating too much friction when the turntable deflects to one side. Of course, such deflection would only occur in the first place if the object were placed way off centre or have a centre of mass far away from the geometrical centre.

One possible explanation for the prototype's higher deflection could be because of the material of the shaft and turntable. Since both the shaft, by accident, and the turntable platform were manufactured from aluminium, they might not be stiff enough to withstand a mass of 20 kg placed at a distance away from the centre. It would be ideal if the turntable were made of a stiffer material like mild steel which has a Young's modulus of 207 GPa compared to 68.9 GPa for Aluminium Alloy's (36). Using a material with a higher Young's modulus would result in a smaller deflection, such as mild steel. This however has the drawback of increasing the total product weight as the density of mild steel is approximately 2.88 times that of aluminium alloy and a turntable platform would weigh 7.7 kg instead of 2.67 kg when made of aluminium (36).

Inexact tolerances would also result in a higher measurement from the dial gauge since the platform and shaft would have space to move about in the bearings or pulleys, resulting in significant tilt. This implied that the j5 shaft tolerances could have exceeded, highlighting the importance of tolerance control the manufacturing process.

Actual deflection on the actual product also is expected to be lesser as a stiffer steel shaft would allow for less turntable tilt. As such, the structural integrity tests have shown that turntable deflection is manageable and will not be an issue.

9.3 Evaluation of Electrical Controls Test

The main findings from the electrical controls test are summarised in Table 16:

Table 16 Summary of electrical controls test results.

Design Aspect	Findings
Angular Displacement	Approximately constant 90° turn observed regardless of weight and load condition, taking about 11 seconds to complete, including settling time
Settling Time	Takes about 2 seconds to settle regardless of weight and load condition
Motor Configuration	Micro step of one-sixteenth with a delay of 40 milliseconds between steps for smooth movement

The turntable was able to rotate to the predefined angle of 90° reliably when it was loaded centrally and only has a percentage error of 1.1%. The scan quality is not affected by the accuracy of the angular displacement as the Iterated Closest Point (ICP) algorithm in CloudCompare does not require an initial angular estimate. The need for positional feedback is therefore not required in our design.

The scaling of rotation time with angle could be considered linear as the low angular velocity implies little time is spent accelerating and decelerating. Hypothetically, if an object required 40 scans with a rotation angle of 9°, the expected rotation time would be about 2.9 seconds, assuming a constant settling time. The total scan time would thus be about 61 minutes, assuming a maximum scan time of 90 seconds from the scanning tests in Section 8.2. Given that geometrically simple objects require at most 10-15 scans, the requirement of scan time under an hour is thus met.

A major issue was encountered when the turntable was loaded off-centre with a 150 N weight. The turntable could not rotate to a full 90° and motor would slip at certain positions. This implied that the torque provided by the turntable is inadequate. To ensure a failproof solution, the turntable must operate regardless of the placement of the object. This would require the torque to be increased to accommodate the loading, which will be discussed in Section 10.2. Further controls test would be required after the torque had been increased to check if the modification has resulted in a sufficient torque.

From the controls test, it was observed that there was some overshoot before the turntable settled to a stop after rotation, increasing the settling time. One solution to this is to implement a PID control for the system. However, the selection of a stepper motor was to eliminate any unnecessary control needed. Hence, a ramp input could be implemented in the Arduino such that the turntable is programmed to slowly increase the speed of rotation from stop to the desired speed and when it is nearing the end of the rotation, decelerate to a stop. This may not completely remove overshoot since the motor still moves in steps, but it will

significantly reduce the extent, and shorten the settling time. Further tests are required to assess the effectiveness of the ramp input.

9.4 Scanning Considerations

The main findings from the scanning attempts are summarised in the Table 17:

Table 17 Summary of scanning test results

Design Aspect	Findings
Environment	Source of lighting needed such that the calibration panel can be seen even at the dark regions of the grey code patterns. If lighting is too intense, the exposure of the camera must be reduced accordingly.
Calibration	A slight movement of the projector and camera can render the calibration parameters invalid, leading to warping of the reconstructed point cloud.
Image Acquisition	The time taken to acquire one set of images was found to be at most two minutes. An object with high reflectivity would not be able to be encoded properly.
Point Cloud Alignment	An object's geometry has a large impact on determining the number of unique views needed to reconstruct a complete point cloud. Objects with sharp corners would need a smaller angular change between views.
Meshing	Screened Poisson Surface Reconstruction was the most optimal method of watertight mesh reconstruction, with a reconstruction depth of at least 14 for sufficient mesh quality.
Hardware Requirements	Control over the camera's exposure and focus settings is needed to ensure the grey code patterns are properly captured. The proportion of space taken up by the object with respect to the projected image has a large bearing on point cloud resolution.

From the results, it is clear that a successful scanner must be able to allow for positional adjustment of the scanning hardware to account for the varying geometries of the scanned object. Furthermore, the user should be able to specify the angular change between rotations, to account for objects with sharper corners or sharp discontinuities. It is also necessary that the mount for the projector and camera must hold these components in place, to prevent invalidation of the calibration parameters.

Hardware testing has also shown that the need for manual exposure and focus control is paramount, which was lacking in the webcam used. The choice of a short throw distance combined with a small screen size was proven to be correct, with the point cloud density far superior than that obtained using the Dr. Q HI-04 projector in the second proof-of-concept test.

Lastly, the point cloud manipulation and alignment software CloudCompare was used to much success, and MeshLab was able to implement the Screened Poisson Surface Reconstruction to mesh the combined point cloud.

10 Design Iteration and Further Development

10.1 Design Considerations

From the prototype evaluation, it is seen that there is a need to improve the torque transmitted by the motor. Having also verified the independent viability of the turntable and

scanner, it is necessary to integrate these components together, where automatic turning occurs after all images have been projected. There is also a need to design a scanner platform, a housing for all electronics and transmission parts, and lighting control for the entire setup.

10.2 Transmission

As the main issue was the lack of sufficient torque, a few solutions were considered, shown in Table 18:

Table 18 Evaluation of possible solutions to increase the torque output.

Solution	Advantages	Disadvantages
Increase Transmission Ratio	Little modification to existing design	Increase in torque with same power results in a slower turning speed
	Lowest expenditure among the solutions	
Increase Motor Torque	Little modification to existing design	Getting a more powerful motor would incur high costs
Replace bearings with self-aligning variants	Reduces bearing friction arising from eccentric loading, reducing torque needed to overcome said friction	Unable to qualify exactly extent of reduction without vigorous testing with product
		Requires major changes to shaft and turntable design, incurring extra costs

An increase in transmission ratio was chosen as the best solution, as new pulleys would cost less than a new motor. With as few changes as possible to the prototype, this allowed our test results such as deflection and structural integrity to still remain valid in the final design.

Another unrelated benefit is the increase in the effective angular resolution of the turntable, as the same number of motor steps input would result in a smaller turntable turn angle.

The issue of slower turning speeds was deemed inconsequential given that small turning angles are needed in SLS, and the actual scanning taking up a majority of the operation time, as shown in Section 8.

While theoretical calculations in Section 7.2.3 showed that the motor torque of 1.89 Nm was sufficient, complex non-linear factors such as plate deflection and bearing friction introduced external resistances to movement. It would thus be more efficient to make an estimate on the required transmission ratio based on current test results.

Given that the test masses were loaded on the edge of the turntable as per Section 8.1.2, to simulate a worst-case scenario, it is reasonable to draw an inference on the needed torque based on the test results obtained. It was shown that for the prototype's 1:1 pulley ratio, an edge loaded mass of 15.29 kg (150 N) caused stalling at certain angular positions while completing the desired turn at other starting positions.

A friction factor α is then estimated, that relates the torque provided by the motor to the actual torque used to move the load, given by the Equation 17 below:

$$T_m = \alpha T_L \quad (17)$$

Where $0 < \alpha < 1$. This factor should account for the resistances to turning due to plate deflection and bearing friction and can be used to estimate the required transmission ratio needed.

This assumes that the motor torque is just enough to turn a certain maximum load, and from the test results can be assumed to be 10.2 kg (100 N) for a conservative estimate, the mass at which full motion without slip was still possible. The value of T_L can be found via the following Equation, assuming a point mass loaded at the turntable edge:

$$T_L = I\ddot{\theta} \quad \text{where } I = I_s + \frac{1}{2}(m_t + 2m_o)R_t^2 \approx \frac{1}{2}(m_t + 2m_o)R_t^2 \quad (18)$$

With m_t and m_o being the masses of the object and the turntable respectively, I_s and R_t being the rotational inertia of the shaft and radius of the turntable. Shaft inertia is ignored given the relative mass and position with respect to the mass of the turntable and the loads, while the load is assumed to be a point load acting on the edge of the turntable.

Using the above equation, the value for $I^{10.2kg} = 0.72 \text{ kgm}^2$. For an edge loaded mass of 20 kg, the inertia is given as $I^{20kg} = 1.33 \text{ kgm}^2$. As the transmission ratio is the ratio of the new motor torque required over the original, and assuming the same initial angular acceleration, the transmission ratio is thus:

$$\text{Transmission Ratio} = \frac{T_m^{20kg}}{T_m^{10.2kg}} = \frac{T_L^{20kg}}{T_L^{10.2kg}} = \frac{I^{20kg}}{I^{10kg}} = 1.85 \quad (19)$$

This assumes linearity of motor to actual torque, which may not be the case when other factors like plate tilt are considered. However, this is useful as an absolute minimum transmission ratio needed. A generous safety factor would also need to be applied given the ambiguities of our friction assumptions.

Ultimately, pulleys of 20 and 80 teeth were selected from HPC's reduced backlash timing pulleys [catalogue](#), where the usage of the same supplier as before meant no or few changes to the pulley width and bores, eliminating the need to modify the existing shaft design.

10.3 Scanner Mount


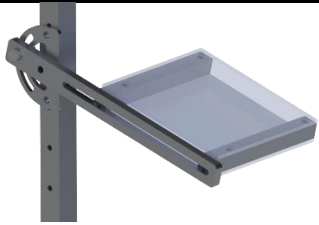
After testing the Structured Light Scanning procedure in Section 8.2, a more complete description of the mount requirements can be defined:

- Due to the varying nature of object sizes, the projector and camera should be able to vary the distance and height from the object in order to ensure the that the object occupies the largest possible space on the screen

- The relative distances and angles between the projector and camera should be adjustable, allowing the user to optimise component placement based on the object geometry

Based on these criteria, the following concepts were developed in Table 19:

Table 19 Evaluation of scanner mount designs.

Concept	Advantages	Disadvantages
 <p><i>Figure 36 Modified Neewer 24-inch tripod to accommodate scanner and projector (37).</i></p>	Keeping the tripod separate from the turntable assembly would reduce transmitted vibrations to the projector and camera	Tripod must be purchased from an external supplier
	Projector and camera are on the same plane, which makes calibration easier	Engineering drawings not provided for tripod parts, which makes modification more difficult
	Tripod has a built-in height and pitch control via knobs, which may help in attaining the optimal scan angle	As the tripod is meant for one camera, further modifications need to be made to accommodate a camera and a scanner
	The distance from the tripod to the scanned object can easily be adjusted	
	Easily portable, can be folded up and kept in a separate bag	
 <p><i>Figure 37 Extendable arm attached to an external frame with pitch control. Camera and projector each require a platform.</i></p>	Cheaper than purchasing a tripod from an external supplier	Requires significant amount of manufacturing Dependent on a robust frame to accommodate two cantilevered supports for a projector and camera More difficult to calibrate scanning system if projector and camera are on separate planes Bulkier, harder to transport and store

The modified tripod design was chosen, as the flexibility in positioning as well as the simplicity of design outweighed the need for additional modifications, which would still likely be faster than manufacturing the extendable arm device.

The ambiguity of dimensions was mitigated partially by the common standard of using a M6 thread to attach to a camera base. As such, the tripod interface was known and could be designed around it. The Neewer Mini 24-inch tripod was chosen due to its height range of 320 – 620 mm, thus allowing vertical adjustments based on the height of the object.

10.4 Lighting Control

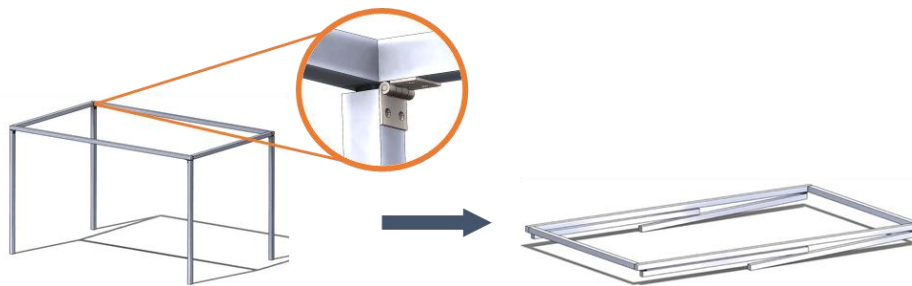


Figure 38 Foldable external frame for ambient lighting control.

The scanning test results has also highlighted a need for a controlled lighting environment. This was to be done using a frame setup, with a fabric covering the frame as shown in the Figure above. The hinges placed along the corners allows for folding, while the top rectangular structure is formed by welding aluminium bars. This allows the frame to be kept in a space-efficient manner, also allowing easy transport of the product.

The use of fabric was also designed in mind for the user to easily modify lighting conditions without extensive effort, as simply draping cloths of different opacity over the setup could achieve the desired effect.

10.5 Electronics

10.5.1 Controller

During the prototyping testing process, an [Arduino Uno Rev3](#) was used to control motor movement. Initially chosen for the ease of prototyping, it was then adapted for use in the actual product. This was done for the following reasons:

- Integrated serial port on the board allowed seamless communication with a computer, allowing the user to control scanning operation at a distance. This also tied in with the image acquisition aspect as images captured were to be saved on a computer for processing, thus the user does not have to operate multiple devices.
- Modular nature of the Arduino Uno allows for future modifications such as remote Bluetooth control or adding a Video Graphics Array (VGA) shield for live feedback
- Space saving capabilities of a circuit board was not important as the turntable subassembly is relatively large.

The [Arduino Proto Shield Rev3](#) was then fitted as a circuit board, allowing electrical components to be placed in a compact and orderly fashion.

From the operational tests in Section 8.1, the Pololu A4988 Stepper Motor Driver was also deemed suitable as a motor controller and would be used in the final product.

10.5.2 Power Supply

As per the PDS in Section 4.2, this product is meant to be operated in Imperial College's Dynamics laboratory or a similar setting. While specialised Direct Current (DC) voltage sources might be present, a requirement for a specific DC voltage supply would be cumbersome for the user to obtain and set up. As such, it is expected to be powered by the standard 230 V, 50 Hz Alternating Current (AC) mains (38).

The Arduino Uno is powered by a 5 V DC input, while the motor driver accepts a range of DC voltages from 8-35 V. There is thus a need to convert the AC power supply to multiple DC voltages. Two types of AC-to-DC converters were considered, a linear regulator and a switched mode power supply.

For a linear regulator, the high AC voltage is reduced via a transformer, then rectified by diodes and smoothed by capacitor to output a low DC voltage (39). A Switched Mode Power Supply (SMPS) on the other hand directly rectifies the high AC voltage to a high DC voltage, which is then stepped down via a switching transistor and smoothed. The advantages and disadvantages of these converters were then considered in the Table below:

Table 20 Comparison of AC to DC converters.

Converter	Advantages	Disadvantages
Switched Mode Power Supply (SMPS)	Much higher efficiencies compared to linear regulators, from 70%-75% (40)	Switching operation introduces high frequency noise that can affect other sensitive devices
	Usually more compact than linear regulators (41)	
	Able to easily accommodate multiple output voltages	
Linear Regulator	Generates little to no electrical noise and fluctuations	Lower efficiencies of 20%-60% (40) due to power dissipation at transformer
		One linear regulator provides only one output voltage

Given the lack of noise-sensitive equipment in our design and the need for two output voltages, a SMPS was determined to be the most appropriate choice.

The chosen power converter, [Mean Well's 54 W SMPS](#), has DC output voltages of 5 V and 12 V, thus able to power both the motor and the Arduino Uno.

10.5.3 Safety Switch and Operational Indication

Also stated in the PDS is the need for the user to know if the device is in operation and a way for the user to stop the operation midway. While the state of the device may be obvious when directly observing the turntable, the presence of the diffuse cloth on the frame would hide the operational state. As such, an alternative way of indicating if the device is on or off would provide explicit information to the user without having to lift the cloth and disrupt the process.

The switch and indication were decided to be independent from the computer both for clarity and simplicity of triggering, as the possibility of computer crashes or delays could hamper the shutdown process.

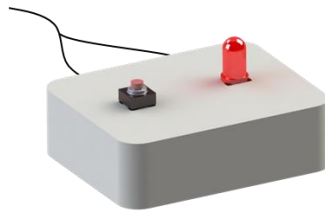


Figure 39 Safety switch and LED.

Actualisation of these two components were in the form of an LED and a button as shown in Figure 39 above, which is then connected to the Arduino Uno. When a button press is registered, the Arduino then halts all processes, sending a signal to turn the LED off.

10.5.4 Layout

The different components of the whole product are split into three distinct groups, the turntable subassembly, the tripod subassembly, and the external components. This can be seen in Figure 40 below, along with the connections between parts.

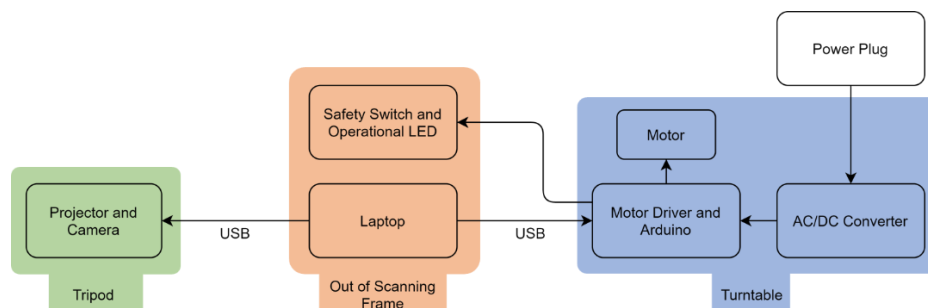


Figure 40 Schematic of entire scanning system.

The projector model uses rechargeable batteries and does not need a power source to operate. The external components comprising of the laptop/computer and the safety switch and LED pair are connected to wires that extend out of the scanning frame.

The schematic of the electronics is shown in Figure 41 below:

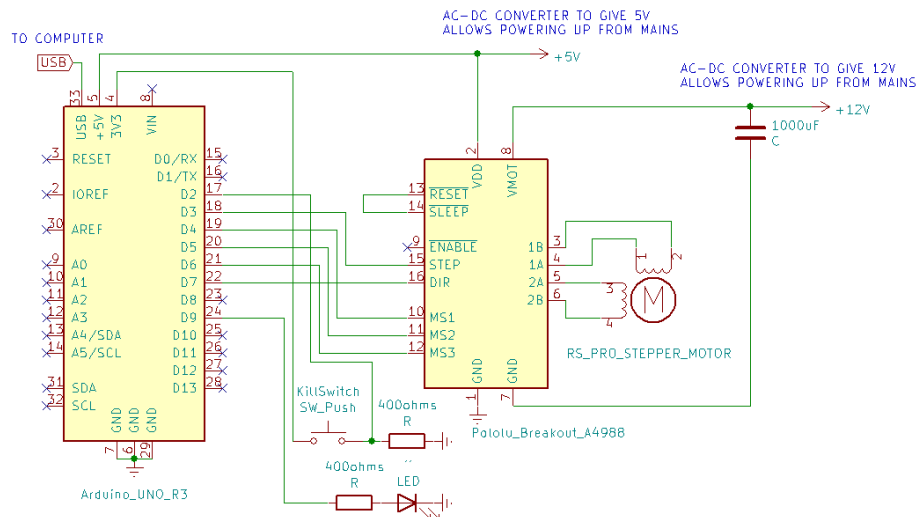


Figure 41 Electronics schematics.

Configuration for the Pololu stepper motor driver and motor is similar to that in Section 8.1.2, and the LED is connected to the Arduino Uno as a digital output while the kill switch is connected as a digital input set as an interrupt. When the switch is depressed, the circuit from closed and an input of 3.3 V is detected, causing the Arduino to send a command to stop all processes.

With all the ancillary components in place, the operational Python script is integrated with the Arduino, with commands being sent out via the Universal Serial Bus (USB) to trigger the motor. The code can be found in the project's GitHub.

10.6 Encapsulation and Covers

There is a need to protect all electrical and transmission parts from moisture, dust, dirt etc. Furthermore, the connecting of wiring away from the turntable such as the USB cables and power cables can serve as potential sources of damage to the product. For instance, if power cables were directly soldered onto the AC-to-DC converter, and accidentally pulling the power cable would damage the connections and potentially cause short circuits. Likewise, the safety switch and operational LED extends out of the scanning setup, and a forceful tug should not damage the Arduino and the shield that it is connected to.

As such both the AC-to-DC converter and the Arduino Uno needs to be covered and their connections protected, such that any excessive force would not damage the critical components.

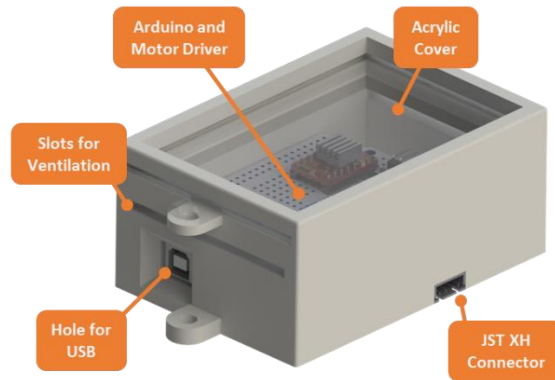


Figure 42 3D printed Arduino and motor driver housing box.

For soldered contacts between components, such as the 12 V and 5 V supplies to the Pololu motor driver and Arduino Uno respectively, the [JST XHP male connector](#) was attached via epoxy to the sides of boxes containing the converter and the Arduino, and wires were soldered connecting the internal components to the connector. The [JST XHP female connector](#) was then soldered onto the ends of external wires to interface with the male connector.

The use of these connectors prevents direct damage to the soldered connections as excessive force would disconnect the connectors first. Also, the assembly and setup process are hastened as the user is not concerned about wiring details and only needs to attach the appropriate connectors.

The boxes themselves, not subjected to any external forces, are simple 3D printed Acrylonitrile Butadiene Styrene (ABS) structures with the relevant holes at the base and open at the top, being covered by a clear acrylic sheet for easy assembly and observation. Slots along the sides of the box allow for ventilation to cool electronics.



Figure 43 3D Printer box for AC-DC converter.

A [Schurter C14 IEC connector \(male\) panel mount](#) is used to interface the mains with the AC-DC converter, as well as provide an on-off switch.

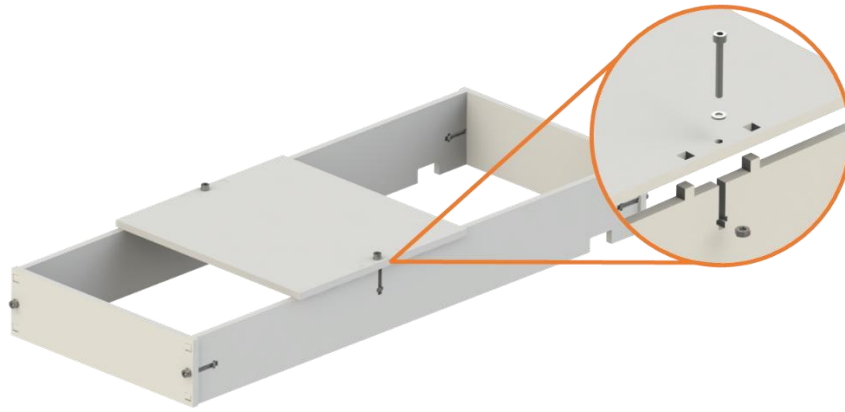


Figure 44 Acrylic transmission cover.

Lastly, the transmission is covered using laser-cut acrylic sheets for an easily assembled and cost-effective solution. The use of T-joints, shown in Figure 44 above, allows fastening at right angles without bulky protrusions or requiring intensive manufacturing.

10.7 Additional Changes

After the initial turntable assembly prototype was manufactured and during testing, it was noted that it was not easy to transport. This was because the baseplate was of a similar size to the turntable, resulting in little room to grip the turntable assembly. In order to address this issue, the base plate was enlarged to accommodate additional electronics as well as two handles to improve transportability.

Holes were also drilled into the turntable to allow for the clamping of irregularly shaped objects which may not exhibit stable equilibrium or may slip when the turntable rotates. While this was not part of the PDS, the addition of holes into the turntable was to ensure that it could be compatible with future use.

11 Manufacturing

The factors considered during component material selection correspond mainly to their relevant applications. The components used in the design were mainly made from Aluminium 6082T6 and Mild Steel EN1A. Majority of the components tended to be made from Aluminium due to its light weight and resistance to corrosion. However, for components pertaining to high strength applications Mild Steel was employed. Since Mild Steel is a relatively denser material it was ensured that the resulting components embody a compact design.

Additional materials employed also include acrylic and ABS plastic pertaining to covers and boxes and were manufactured using CNC services provided by the STW.

Manufacturing methods used were mainly restricted to those available in the student teaching workshop (STW). These can be divided into CNC and manual methods which have been summarised in Table 21.

Table 21 Methods used to manufacture parts in the STW.

Methods	Components
CNC Turning	Turntable Shaft, Idler Shaft, Bearing Housing
Laser Cutting (Metal)	Turntable, Base Plate, Intermediate Plate, Motor Plate
Additive Manufacturing (3-D Printing)	Arduino & Convertor encasing
Laser Cutting (Acrylic)	Transmission covers
Manual Turning	Transmission components (i.e. spacers, pillars, etc.)
Welding	Frames
Threading	Pillars
Drilling	Pillars, Plates, Turntable etc.

12 Final Design

The final design can be divided into 3 separate sub-assemblies: Scanning, transmission, and the light control frame. All three of these sub-assemblies are physically separated from one another and are integrated during operation.

12.1 Scanning Assembly

The scanning assembly mainly consists of 3 main components: Camera, Projector and Tripod.



Figure 45 Modified scanner mount to accommodate a projector and webcam.

The projector used is the [AAXA P300 Neo Projector](#), while the camera is the [Logitech C920 Webcam](#). The detailed specifications can be found in Section 8.2.2.3 or at the manufacturer's website. While hardware testing has shown that the webcam is inadequate in the context of SLS, the scanner mount has been configured such that different camera models can easily replace it.

As mentioned in the previous Section, M6 screw threads are a common standard for photography-tripod connections, thus the equally spaced M6 clearance holes on the mount

allows components to be easily swapped out and fastened via a bolt. These holes also allow for easy changing of component distance based on scanning requirements.

This mount interfaces with the tripod by fastening onto a slider plate using 2 bolts, restricting any rotary movement thereby ensuring a rigid scanning assembly structure following calibration. The slider is press-fitted onto the tripod mount, shown in Figure 45 above.

12.2 Transmission Assembly

The transmission sub-assembly is comprised of both mechanical and control segments. The mechanical segment consists of a series of manufactured components as well as externally purchased parts whereas the control segment helps facilitate the mechanical motion within the transmission system. Both these segments together bring about a controlled, stepwise angular rotation of the object being scanned.

12.2.1 Turntable

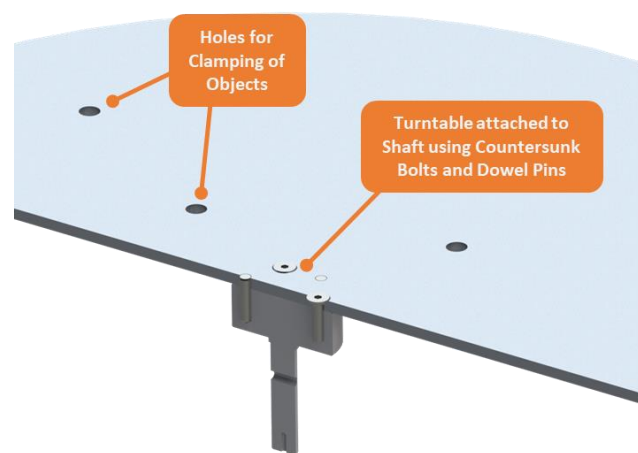
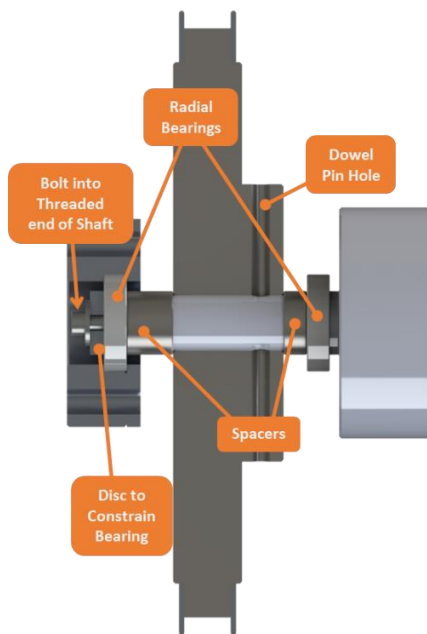


Figure 46 Section view of turntable.

The turntable was manufactured from a 5 mm thick aluminium sheet, with countersunk bolts to hold it axially to the shaft and dowel pins to transmit torque.

12.2.2 Turntable Shaft



The turntable shaft supports the turntable along with the object load placed on it. The shaft is made from mild steel to meet the high strength requirements against bending, buckling and torsion thus manifesting a more stable operating performance.

The left bearing is axially constrained with a steel disc held in place by a bolt screwed into the threaded end of the shaft, while the right bearing is held radially by an intermediate plate of the same thickness as shown in Figure 47.

Figure 47 Section view of turntable shaft

12.2.3 Pulley & Belt

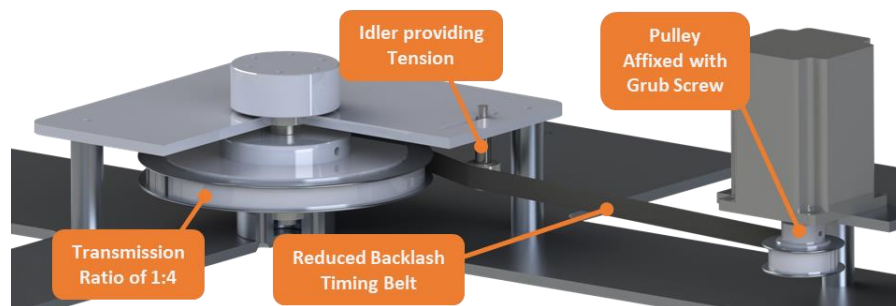


Figure 48 4:1 Belt and pulley transmission.

Figure 48 above shows the selected transmission mechanism connecting the motor and the turntable, with both the pulleys and belts purchased from HPC.

12.2.4 Base Layout & Transportability

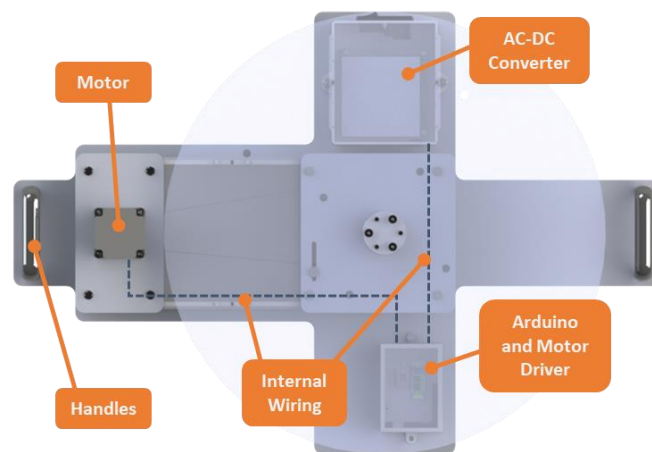


Figure 49 Overview of base plate and electrical wiring layout.

The entire transmission assembly is attached to the base plate. The base plate area was redesigned as a cross to minimise weight but still provide stability and space for the electronic components. Handles have been attached onto the sides of the base plate to improve transportability. Dotted lines in Figure 49 above shows how the wires are to be laid out on the base plate, connecting the electrical components together.

12.3 Overall Assembly

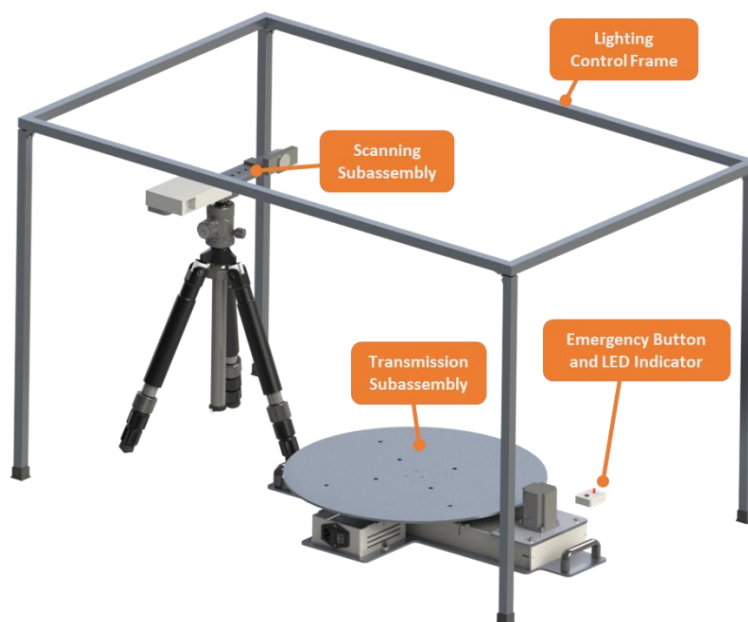


Figure 50 Overall setup of the entire scanning system.

Figure 50 above shows the entire assembly with individual subassemblies. Rubber caps were also installed on the legs of the frame to prevent scratches on the floor and improve grip.

A frame cloth was also intended initially to cover the entire system. The cloth would act to control light entering the assembly as per the requirements of the scanning set up. However, due to the abrupt college closure, the cloth could not be procured in time.

The total mass of the assembly was estimated from Solidworks to be 17.7 kg, and thus fulfils the PDS criteria of being under 30 kg for easy transport.

12.4 Engineering Analysis

The lifetime of the product mainly depends on the components used. This section focuses on the main failure modes of some of these critical components and giving an overall judgment from an engineering perspective with regards to the requirements specified in the PDF.

12.4.1 Shaft Stress Calculations

The shaft is the component most prone to failure in the entire system. Using equations from Section 7.2.4 and accounting for the increase in the transmission ratio, the new shaft safety factor was calculated. The only change resulting from this pertained to the belt pull force thus increasing the bending moment value in Equation 5. The new bending moment value calculated was 2.77 Nm and the resulting σ_{max} obtained was 42.63 MPa.

The safety factor thus obtained according to the Von Mises criterion was:

$$S.F. = \frac{\sigma_{yield}}{\sigma_{max}} = 5.4 \quad (20)$$

12.4.2 Fatigue Analysis

The PDS suggests a service life of 5 years. Assuming the operational speed of the turntable is 1RPM and on average the system is in operation for 2 hours per week. This leads to 28800 turntable revolutions over a 5-year period. The number of cycles to failure should be greater than this value to meet the service life criteria specified in the PDF.

The Basquin Equation (42) is used to estimate the cycles to failure from the S-N curve for the high cycle fatigue region.

$$N = \left(\frac{\sigma_a}{a} \right)^{1/b} \quad (21)$$

where N is the number of cycles to failure and σ_a is the stress amplitude. a and b are empirical constants found using the assumptions stated below (43).

- **Assumption 1:** when $N = 10^3$, σ_F is equal to $0.9\sigma_{UTS}$. This assumption is based off the S-N curve behaviour in the low cycle region.
- **Assumption 2:** when $N = 10^6$, σ_F is equal to the fatigue limit σ_e .

Substituting the above assumptions into Equation 21 and taking the log of both sides, the following equations are obtained:

$$\log(0.9\sigma_{UTS}) = \log(a) + 3b \quad (22)$$

$$\log(\sigma_e) = \log(a) + 6b \quad (23)$$

Rearranging gives:

$$a = \frac{\sigma_e}{10^{6b}} \quad (24)$$

$$b = \frac{\log(\sigma_e) - \log(0.9\sigma_{UTS})}{3} \quad (25)$$

Calculating an exact value for σ_e was out of the scope of this project thus it was assumed that it is equal to $0.5\sigma_{UTS}$ for σ_{UTS} values less than $1,000MPa$ (42). The σ_{UTS} value for mild steel used is $370MPa$ (20). Substituting these values in Equations 24 and 25 gives a & b values of $599.5 MPa$ and -0.085 .

The σ_a value used is the σ_{max} value $42.63 MPa$. This is due to the shaft being subject to continuous step wise rotations, resulting from the holding torque applied continuously by the motor. Hence, maximum load conditions were used in this case rather than operating conditions.

Using these a & b values in Equation 21 gives an N value of 8.78×10^{12} cycles to failure. This value is significantly greater than the N value required to meet the service life thus confirming the integrity of the shaft design.

12.4.3 Bearings

Bearings were used on the shaft to ensure the shaft is accurately placed without any tilt. The performance of the bearing will affect the turntable rotation and thus the scan therefore it is vital that these bearings perform to ensure accurate scan quality.

The L_{10} value of the bearing was found using the following equation:

$$L_{10} = \left(\frac{C}{F}\right)^k \times 10^6 \quad (26)$$

The dynamic load rating (C) for the bearing given is $1.43 kN$ (44). The constant k was considered as 3 for ball bearings (45). F was found using Equation 27.

$$F = XF_r + YF_a \quad (27)$$

The axial force F_a acting on the table is approximately $200N$ and the F_r value obtained using methods employed in the previous section was $425.9N$. Thus, the X and Y values obtained from the tables were 0.56 and 1.26 (45). This resulted in an F value of $490.50N$. Substituting these values in equation x gives an L_{10} rating of 24.8×10^6 revolutions.

Based on a service life of 28,800 cycles to failure, this L_{10} value more than suffices in meeting the design lifetime criteria specified in the PDS.

13 Project Budget

This section entails a summary of the financial expenditures that occurred throughout the course of the project. A breakdown of the individual section expenditure can be found in Table 22. Expenditures in the prototype section correspond to components that could not be used in the final assembly.

Table 22 Summary of planned and actual expenditure.

Budget Assigned	Amount Allocated (£)	Spent (£)
Scanning System	400	384.92
Transmission	200	187.16
Raw Materials	150	113.75
Control	100	153.67
Prototyping	150	153.58

Expenditure went over budget in the Control section. This resulted due to the failure in anticipating the high cost of the motor and additional electrical related equipment required in supporting the control system of the assembly (e.g. Male-female Connector, PCB, etc.). The prototype related expenses were also seen to go over budget. This was mainly due to major design changes after prototype testing thus nullifying a significant portion of the components used in the prototype assembly.

The total amount spent towards the end of the project amounted to £ 993.08. Additionally, due to early college closures, arising from the pandemic, the costs pertaining to ME-Stores had to be estimated as no pro forma invoices could be generated in time. While estimating, it was ensured that costs were rounded up where reasonable. Assuming the estimates are relatively accurate, and no additional expenses are incurred, it can be stated that the project is just within budget.

14 Alternative Work Package

14.1 Background

On the 15th of March (Sunday), the college made the decision to switch to remote teaching by the 18th (Wednesday), due to the outbreak of COVID-19 within Imperial College's community. As such, the college was to close on the 17th of March. A follow up email by the Mechanical Engineering department notified all staff and students that closure of all laboratories and workspaces was to be done by 3pm of the 17th, and DMT projects would be submitted as it is, with manufacturing and testing plans that week to be cancelled.

As the shutdown of campus meant that no further work could be done on the actual product, an Alternative Work Package (AWP) scheme was implemented in place of work that could not be completed. The AWP was dependent on both the group's remaining progress and what resources the members had at hand.

14.1.1 Affected Tasks

From the project timeline in Section 4.5, the original intent was to test of our final product in the week of 16th – 20th March, coincidentally the last week of school before the Easter break. This one week of was also allotted as slack on manufacturing. Fortunately, manufacturing was started a week earlier on the 9th of March, and as a result the completed product was manufactured, sans the fabric to control lighting. However, we were unable to carry out operational and structural tests on the final product. A full list of the intended tests is shown in Table 23:

Table 23 Summary of product testing status.

PDS Objective	Test	Status
Scanner Output	Integrated test of turntable and scanner operation	Not carried out, but components work separately
Scan Time		
3D Model Resolution	Scan an object with known dimensions, and compare the obtained model	Not carried out, no precise measurement tools available out of college
Scan Volume	Turntable structural integrity test for a 20 kg object loaded eccentrically	Not carried out, but results from prototype can be used given lack of changes to turntable material
	Electrical control test for a 20 kg object loaded eccentrically	Not carried out
Operational Safety	Kill-switch testing and LED indicator status check	Not carried out on complete product, but individual functionality tested during assembly
Transportability	User feedback from moving scanner through different routes	Not carried out

14.1.2 Work Scope

Our team proposed the following task, which was accepted by the supervisors:

- Devise and conduct further tests to investigate optimal Structured Light Scanning conditions, which can be done by varying the scanning environment or surface conditions of the scanned object.

After some consideration, we decided to investigate the scanning of reflective surfaces as prior testing in Section 8.2 has shown that scan quality greatly deteriorates when the object is highly reflective. This is especially relevant in the context of the Dynamics lab, where the majority of engine components are metallic and smooth, such as the blades of a compressor or the shell of a turbine. As such, determining the optimum procedure to scan shiny objects would be the most beneficial choice.

14.2 Considerations

The effect of surface roughness on encoding quality can be explained by considering the behaviour of the reflected rays. A matte surface causes light rays to be reflected at randomly scattered angles, known as a diffuse reflection (46). As such, the intensity of rays reaching the camera across the whole surface is generally rather uniform, allowing all features to be captured. On the other hand, a smooth surface tends to reflect most light rays along a narrow set of directions at the same incident angle to the light source, known as specular reflection. With a direct source of light, there will be an angle at which a much higher intensity of light is reflected, and that is the source of glare when photographing shiny objects. This localised intensity in a photograph can then obscure the surrounding features, and thus the grey code patterns will not be properly represented.

In the context of SLS, there are two common ways of eliminating glare; Diffuse the lighting conditions such that there is no direct source of light or making a smooth surface 'rough'. The former is achieved either by removing the direct light sources or diffusing lighting via translucent cloth. There are multiple ways to achieve the latter, such as painting the surface with a matte substance or by sanding it.

It is impossible to eliminate a direct light source, given that the projector itself acts as one and cannot be diffused without distorting the patterns. As such, surface modification techniques will be tested instead.

14.3 Methodology

A common method used by commercial solutions, to deal with reflective surfaces is to use specialised sprays, such as [3D Scanning Developer Spray](#) or [AESUB Blue](#), that deposit a finely dispersed layer of particles that effectively creates a matte layer without significantly affecting surface features. Such sprays are often used in crack detection or surface damage surveillance systems as well.

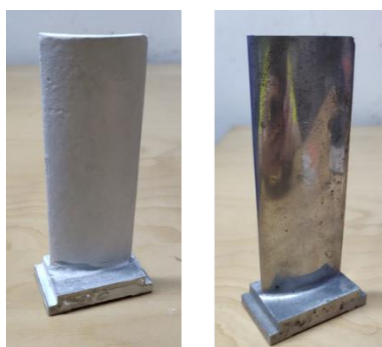


Figure 51 Coated and uncoated turbine blade.

The spray was emulated by a mixture of [baby powder](#) and 70% isopropyl alcohol. Baby powder consists mostly of fine unreactive talc, which would be suitable as an easily cleaned coating. Baby powder and the alcohol is mixed with a 1:3 ratio in a spray bottle. The result of the applied spray on a shiny object is shown in Figure 51 above.

The SLS scan is attempted on the above object both with and without the applied spray, with the same set up and procedure as detailed in Section 8.2.1. The equipment used is the AAXA P300 Neo Projector and a OnePlus 6T Android phone. The specifications of both can be found in Section 8.2.2.3.

14.4 Results

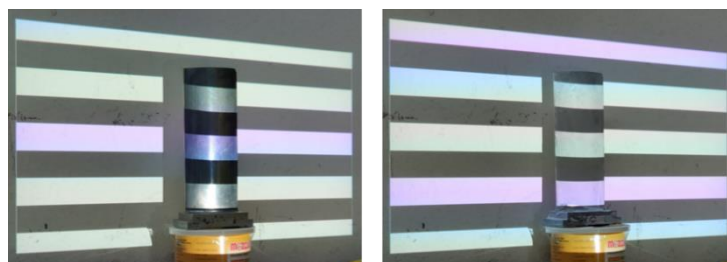


Figure 52 Uncoated and coated turbine blade during scanning.

During the scanning process, the pixel bloom issue, shown in the left image of Figure 53, is largely eliminated when coated, allowing patterns to be properly registered.

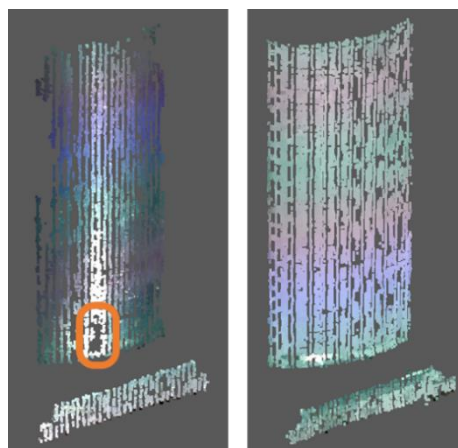


Figure 53 Frontal scan of the uncoated and coated blade

Figure 53 above shows the frontal scans of the uncoated and coated blade. A visual inspection shows more gaps in the uncoated model, with a lack of points at the region corresponding to the greatest light intensity in the previous Figure 52. There is also a lack of points around the blade edges.

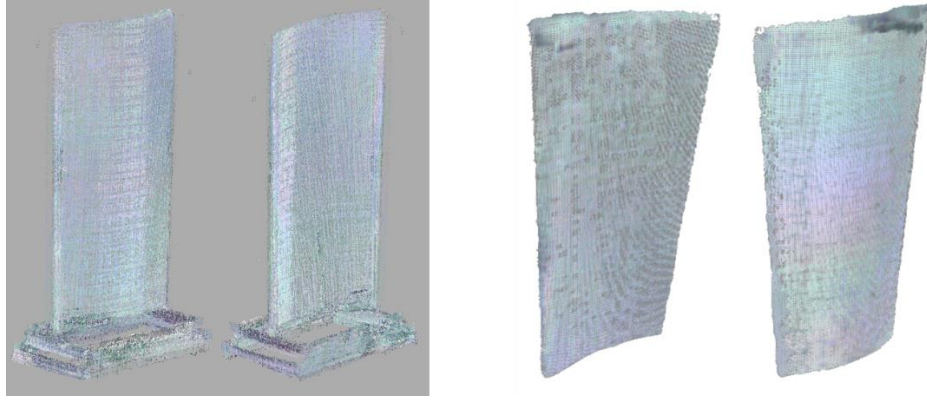


Figure 54 (left) Fully aligned point clouds of the blade, (right) Mesh of coated and uncoated turbine blades.

In addition, a total of 24 scans of the coated blade was taken from all angles and aligned to form a complete point cloud and mesh, shown in the images of Figure 54. As seen, the features of the blade appear to be accurately represented with the exception of the thin blade edges.

14.5 Analysis and Discussion

In order to quantify exactly how effective such a coating can be, two metrics were introduced, the total number of points in a single scan, and the distance distribution for every point. It is important that the object position in both scans are the same, so the same features and total area taken up by the object remains the same. For instance, an object closer to the projector would naturally contain more points due to the greater amount of space taken up and introduce another variable into the test.

The distance distribution was obtained via Python's *scikit-learn* nearest neighbour module, after which outliers, noisy points due to uneven spraying or encoding errors, are then filtered out.

Filtering was done firstly by finding the robust z-score (47) for each distance in the set:

$$M_i = \frac{0.6745|x_i - \tilde{x}|}{MAD} \quad (28)$$

$$MAD = median\{|x_i - \tilde{x}|\} \quad (29)$$

Where *MAD* stands for the median of the absolute deviation, and \tilde{x} is the median distance of the set. This robust z-score is used over a standard z-score to avoid the influence of outliers. Distances with this robust z-score of greater than 3.5 is then considered an outlier and eliminated, and the remaining plotted as a histogram.

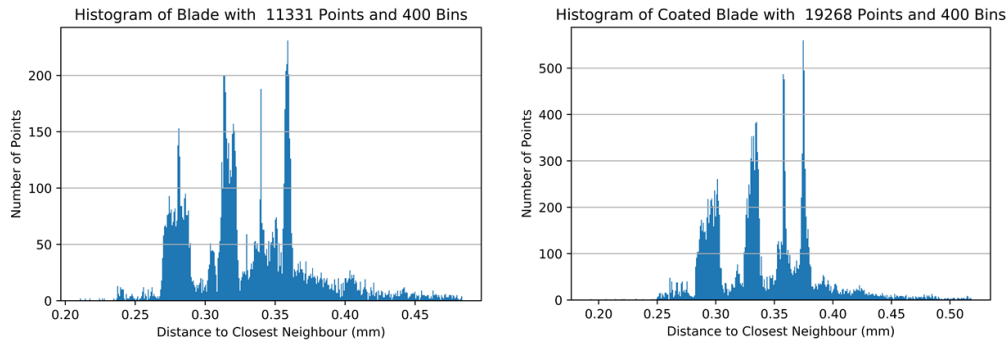


Figure 55 Distance between individual data points for an uncoated and coated turbine blade.

Figure 55 above shows the distance distribution of the uncoated and coated blade, as well as the total number of points. It is seen that the application of the coat increases point count by about 70.0%. The lower cut-off distance for scans are roughly the same and is limited by the resolution of the camera and projector, and the distribution of distances appear approximately the same. This similar distribution shows that even though the uncoated scan is sparser, these points appear as clusters, thus the distance to the closest neighbour does not change by much.

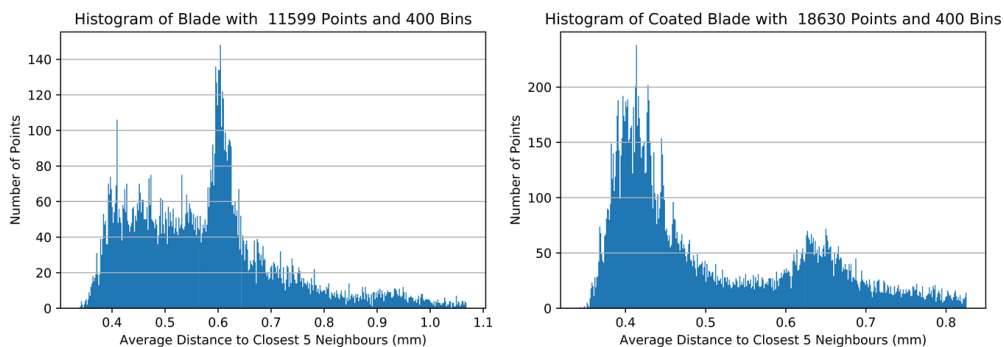


Figure 56 Average distance between individual points for an uncoated and coated turbine blade.

By taking an average distance of neighbours around a point, the clustering of points is less of an issue, allowing clearer patterns to be seen between the two scans. The Figure 56 above now shows the average distance of the five nearest neighbours to each point instead. From the above figures, it is seen that the uncoated blade has a distribution mostly within 0.4 – 0.6 mm, with a local median at 0.6 mm. On the other hand, the coated blade's distribution centres mostly about a distance of 0.4 mm, with a secondary peak at about 0.6 mm. On average, most points obtained from the coated blade are more tightly packed compared to the uncoated blade.

From this analysis, the results of such a coating can be deemed to be effective in increasing the point cloud density and reducing encoding errors. Furthermore, this method allows one to

scan transparent or translucent objects too. One drawback is that markings can become obscured, which may make alignment more of an issue for symmetrical objects.

The issue with scanning and reconstructing geometrically thin objects persists however, as seen in the complete mesh in Figure 54 above. This could be rectified with using a projector of higher resolution or taking more scans at the areas of large angular changes.

15 Future Improvements

The stitching process can be time-consuming and arduous. Manual stitching requires inputting reference points for meshes to assimilate to and hence, the process may also be prone to human error. Many existing scanning solutions such as Matter and Form and Einscan-SE often come with automatic dedicated alignment software for the construction of 3D point cloud of scanned objects.

This convenience is however not available in our current design due to our project scope and timeline. Hence, users are required to perform manual stitching of meshes on Meshlab and CloudCompare to complete the full 3D profile. A future improvement can be to offer an end-to-end, automated approach to the scanning process whereby a user places the object on the turntable, starts the scanning and from the scans, a full 3D object formed without the need for manual processing.

Automation of this process can be achieved by point cloud registration and there are several methods available. An example of this would be to use the Iterative Closest Point (ICP) (48) algorithm instead as a script, where a rigid registration of the points is done in an iterative manner to find the optimal mapping between these point clouds. Translation and rotation are then performed on one point cloud such that a minimum distance between the two clouds is attained. This algorithm if implemented into the workflow would allow for automated stitching of point clouds, increasing ease of processing.

The current design also only incorporates a single camera with a projector to capture scans. However, more cameras can be added into the system to allow for greater coverage of the object and therefore more details can be captured. As more points on the object are collected, fewer scans are needed to fully reconstruct the object, decreasing the scan time.

Another direction for improvement is to use a video feed to capture the encoding patterns, allowing all patterns to be cycled at frequencies close to the video frame rate. This speeds up the process at least tenfold but requires a video recorder with sufficiently high resolution to fully capture these patterns.

There were various manufacturing concerns such as budget and availability of equipment and materials. When designing the overall frame to cover the turntable and scanning device, we found that manufacturing the frame out of aluminium was the most straightforward and cost-effective way. Although it satisfies the design requirements of being portable and to encompass the whole system, the frame can be made lighter by using plastic for each of the components since it is not structurally loaded. Injection moulding of the plastic would however present a higher cost for the project especially when only a small quantity is required. This option can be employed if the design is mass-produced or when more budget is allocated.

16 Conclusion

The final product constitutes of a scanning system that can generate a 3D point cloud of an object under pre-set conditions. This system will be used by the Dynamics Lab group to create CAD Models for engine components. The unique selling point of this design in comparison to the market pertains to its low cost and high modularity. This was the result of the scanning method employed requiring a relatively simple transmission system to collect data which would then be processed, using a complex series of software related operations.

Failure analysis has been conducted on the transmission system, especially on the shaft, to ensure it is designed to avert any arising failure modes with a reasonable safety factor. With respect to the scanning system, the set up does require pre-calibration and the obtained data must be manually processed afterwards. Automating the software process may significantly ease user operation however was deemed beyond the scope of this project.

Due to the Covid-19 crisis and early college closures, strict testing procedures required to validate all PDS criteria could not be completed. However, prototype testing on a structurally similar transmission has validated the structural integrity and control scheme, and scanning tests have successfully produced 3D models in the desired file formats. These results could thus plausibly be used to conclude success on these aspects of the Product Design Specification.

Prototype testing also indicated an inability to move eccentrically loaded weights of more than 100 N, which was rectified by increasing the transmission ratio from 1:1 to 1:4. However, this has not been experimentally verified due to the closures.

Achieving a resolution within 0.5 mm was not experimentally possible with the Logitech C920. However, it has been shown that incorporating a higher resolution camera with exposure and focus control allows relevant features to be reproduced with recognizable detail. Given the

high modular nature of the system, an upgrade in the scanning assembly is easily viable thus allowing this criterion to be fulfilled as well.

17 References

-
- (1) Karwowski W. Maximum Load Lifting Capacity of Males and Females in Teamwork. *Proceedings of the Human Factors Society Annual Meeting*. 1988; 32 (11): 680-682. Available from: doi: 10.1518/107118188786762621 Available from: <https://doi.org/10.1518/107118188786762621> .
 - (2) Tan J, Lim SH, Tiong CS, Ahmez A, Siddiquey H. *Project Quality Plan V9*. London: 2020.
 - (3) TE Halterman. *Eora 3D Unveils \$199 iPhone-powered 3D Laser Scanner*. Available from: <https://3dprint.com/86324/eora-3d-unveils-199-iphone-powered-3d-laser-scanner/> [Accessed 27/05/2020].
 - (4) Matter and Form. *Matter and Form 3D Desktop Scanner*. Available from: <https://matterandform.net/scanner> [Accessed 25/05/2020].
 - (5) Einscan. *EinScan-SE Powerful Desktop 3D Scanner*. Available from: <https://www.einscan.com/desktop-3d-scanners/einscan-se/> [Accessed 27/05/2020].
 - (6) Peel3D. *3D Scanner Handheld Peel 1 Affordable*. Available from: <https://peel-3d.com/products/peel-3d-scanner> [Accessed 27/05/2020].
 - (7) GOM. *ATOS ScanBox Series 4*. Available from: <https://www.gom.com/metrology-systems/atos-scanbox/atos-scanbox-series-4.html> [Accessed 27/05/2020].
 - (8) Bell T, Li B, Zhang S. *Structured Light Techniques and Applications*. 2016. Available from: <https://doi.org/10.1002/047134608X.W8298> .
 - (9) Bagci E. *Reverse engineering applications for recovery of broken or worn parts and re-manufacturing: Three case studies*. 2009. Available from: <http://www.sciencedirect.com/science/article/pii/S0965997808001312> .
 - (10) Corrigan F. *Flash Lidar Time of Flight (ToF) Camera Sensors On Drones And 10 Terrific Uses*. Available from: <https://www.dronezon.com/learn-about-drones-quadcopters/best-uses-for-time-of-flight-tof-camera-depth-sensor-technology-in-drones-or-ground-based/> [Accessed 28/05/2020].
 - (11) Advanced Scientific Concepts Inc. *Technology Overview*. Available from: <http://www.advancedscientificconcepts.com/technology/technology.html> [Accessed 29/05/2020].
 - (12) Pastorius W. *STRUCTURED LIGHT VS. LASER TRIANGULATION FOR 3D SCANNING AND INSPECTION*. Available from: <https://lmi3d.com/company/digital-hub/blog/structured-light-vs-laser-triangulation-3d-scanning-and-inspection> [Accessed 29/05/2020].
 - (13) Borlin N. *Fundamentals of Photogrammetry*. Available from: https://www8.cs.umu.se/kurser/5DV115/VT14/handouts/fundamentals_of_photogrammetry.pdf [Accessed 30/05/2020].
 - (14) Tan J, Lim SH, Tiong CS, Ahmed A, Siddiquey H. *3D Dynoscan Progress Report*. London: 2020.
 - (15) González MÁ, Aramendi J, González-Aguilera D, Yravedra J. Statistical Comparison between Low-Cost Methods for 3D Characterization of Cut-Marks on Bones. *Remote Sensing*. 2017; 9 873. Available from: doi: 10.3390/rs9090873 .
 - (16) RS. *RS PRO Hybrid, Permanent Magnet Stepper Motor 1.8°, 1.89Nm, 3.2 V, 2.8 A, 4 Wires*. Available from: RS PRO Hybrid, Permanent Magnet Stepper Motor 1.8°, 1.89Nm, 3.2 V, 2.8 A, 4 Wires [Accessed 31/05/2020].
 - (17) Johantgen N. *Choosing a step motor: Real example*. Available from: <https://www.machinedesign.com/motors-drives/article/21827541/choosing-a-step-motor-real-example> [Accessed 31/05/2020].

- (18) Knight B. *Understanding Inertia Ratio and Its Effect On Machine Performance*. Illinois: 2015.
- (19) HPC. *Timing belts, formulae, terms & definitions*. Available from: https://www.hpcgears.com/pdf_c33/27.17-27.47.pdf [Accessed 31/05/2020].
- (20) Metals4u. *EN1A Mild Steel*. Available from: <https://www.metals4u.co.uk/blog/en1a-mild-steel> [Accessed 31/05/2020].
- (21) Aalco. *Aluminium Alloy*. Available from: http://www.aalco.co.uk/datasheets/Aluminium-Alloy-5251-H22-Sheet-and-Plate_150.ashx [Accessed 29/05/2020].
- (22) Sturm P. Pinhole Camera Model. In: Ikeuchi K. (ed.) *Computer Vision: A Reference Guide*. Boston, MA: Springer US; 2014. pp. 610-613.
- (23) Lanman D, Taubin G. Build your own 3D scanner. *ACM SIGGRAPH 2009 Courses* : ACM; Aug 3, 2009. pp. 1-94. Available from: <http://dl.acm.org/citation.cfm?id=1667247>. Available from: 10.1145/1667239.1667247.
- (24) Zhang S, Huang P. Novel method for structured light system calibration. *Optical Engineering - OPT ENG*. 2006; 45 Available from: doi: 10.1117/1.2336196 .
- (25) Moreno D, Taubin G. *Simple, Accurate, and Robust Projector-Camera Calibration*. ; 2012.
- (26) Hesamh. *DIY 3D Scanner Based on Structured Light and Stereo Vision in Python Language*. Available from: <https://www.instructables.com/id/DIY-3D-scanner-based-on-structured-light-and-stere/> [Accessed 25/05/2020].
- (27) Johnson K. *Working on High Quality Low Cost DIY 3D Scanning using Structured Light*. Available from: <https://www.cnx-software.com/2018/04/26/working-on-high-quality-low-cost-diy-3d-scanning-using-structured-light/> [Accessed 26/05/2020].
- (28) Matlab. *Supported Hardware – Industry Standard – Generic Interfaces (Webcams)*. Available from: <https://uk.mathworks.com/products/image-acquisition/supported/generic-interfaces-webcams.html> [Accessed 11/05/2020].
- (29) Pololu. *A4988 Stepper Motor Driver Carrier*. Available from: <https://www.pololu.com/product/1182> [Accessed 01/05/2020].
- (30) Bercovich A. *gPhoto*. Available from: <http://www.gphoto.org/> [Accessed 17/05/2020].
- (31) Moffat A. *sh*. Available from: <http://amoffat.github.io/sh/> [Accessed 19 March 2020].
- (32) Khlebovich P. *IP Webcam - Apps on Google Play*. Available from: https://play.google.com/store/apps/details?id=com.pas.webcam&hl=en_SG [Accessed 10 February 2020].
- (33) The Python Software Foundation. *urllib — URL handling modules*. Available from: <https://docs.python.org/3/library/urllib.html> [Accessed 27/05/2020].
- (34) Dai JS. *Euler–Rodrigues formula variations, quaternion conjugation and intrinsic connections*. 2015. Available from: <http://www.sciencedirect.com/science/article/pii/S0094114X15000415> .
- (35) Kazhdan M, Hoppe H. Screened poisson surface reconstruction. *ACM Transactions on Graphics*. 2013; 32 (3): 1-13. Available from: <https://dl.acm.org/doi/10.1145/2487228.2487237> .
- (36) Department of Mechanical Engineering Imperial College London. *Mechanical Engineering Data and Formulae*. London: Imperial College London; 2015.
- (37) Neewer. *Neewer Mini 24 inches/62 centimeters Travel Tabletop Camera Tripod*. Available from: <https://neewer.com/products/tripods-10090907> [Accessed 11 February 2020].
- (38) UK Legislation. *The Electricity Safety, Quality and Continuity Regulations 2002*. Available from: <http://www.legislation.gov.uk/ukxi/2002/2665/regulation/27/made> [Accessed 30/05/2020].
- (39) Winder S. *Chapter 4 - Linear Power Supplies*. Newnes; 2017. Available from: <http://www.sciencedirect.com/science/article/pii/B9780081009253000045> .
- (40) Lai YM. *20 - Power Supplies*. Butterworth-Heinemann; 2018. Available from: <http://www.sciencedirect.com/science/article/pii/B9780128114070000222> .

- (41) Sattel S. *Linear Regulated vs. Switch Mode Power Supply*. Available from: <https://www.autodesk.com/products/eagle/blog/linear-regulated-vs-switch-mode-power-supply/> [Accessed 01/03/2020].
- (42) Davies C. Properties of Engineering Materials – Failure by Yielding, Fracture, Creep and Fatigue. In: Davies C. (ed.) *ME2 Materials*. London: Imperial College London; 2017. pp. 68-73.
- (43) Zorowski CF. *Design for strength*. Available from: <http://www.designforstrength.com/chapter-08.pdf> [Accessed 19/01/2020].
- (44) SKF. *Deep groove ball bearings, single row, seal on both sides*. Available from: <https://docs.rs-online.com/3a16/0900766b80f8ce33.pdf> [Accessed 31/05/2020].
- (45) Childs P. *Mechanical Design*. 2nd ed. Oxford: Arnold; 2004.
- (46) Choudhury AKR. 2 - *Object appearance and colour*. Woodhead Publishing; 2014. Available from: <http://www.sciencedirect.com/science/article/pii/B9780857092298500024>.
- (47) Rousseeuw PJ, Hubert M. Robust statistics for outlier detection. *WIREs Data Mining and Knowledge Discovery*. 2011; 1 (1): 73-79. Available from: doi: 10.1002/widm.2 Available from: <https://doi.org/10.1002/widm.2>.
- (48) Procházková J, Martišek D. *Notes on Iterative Closest Point Algorithm*. ; 2018.

18 Individual Reflections

18.1 Siew Han

The DynoScan 3D project was a tough but rewarding project. Yet akin to running a marathon, it was mostly tough, and only after can one better appreciate what was learnt. As a mechanical engineer, implementing 3D scanning was something I had never done before, and I was plagued by serious doubts throughout each stage of the project. Yet our team pulled through, and an actual product was delivered. While I would like to assert that everything is working and all goals were met, the extraordinary circumstances has led to a great deal of ambiguity in how close we are to the PDS objectives. However, I am confident that we have done quality work, and come off all the better for it.

As the software lead, I was in charge of gathering resources and setting a direction for image acquisition, scanning, reconstruction, and post processing. Yet with little experience in this field, it initially felt like the blind leading the blind, somewhat exacerbated by the glut of information online. Personally, one of the toughest parts of this project was committing to a certain method or procedure, being fully accountable for my choices with little for backpedalling when things go south. And I did run into a lot of dead ends, such as spending a whole night trying to implement a reconstruction technique and getting no headway whatsoever.

But in retrospect, these frustrations and walls made me a more resourceful, more well-rounded engineer. For instance, I was having trouble with a calibration process, and given the

nature of this project, could not seek a subject matter expert in Imperial College. This led to me emailing the academic who pioneered that process for practical help, who offered invaluable advice.

On the managerial aspect, I was the report lead, providing a general flow and allocating relevant work to other members. I found it very easy to conflate what I want with what I think is right and could potentially stifle relevant suggestions had I been dogmatic with my report structures. For me, I believe this comes from my strong investment in the project's success, and I learnt to divest a little in order to appreciate the dissenting opinions as chances to learn. The spread of COVID-19 leading to college shutdown has made me better appreciate the need for contingency planning, as I felt that we were all quite blindsided by the sudden turn of events. Similarly, it is important to avoid an overreliance of some aspects on a single member, as bottlenecks could occur were that member suddenly be unavailable.

As someone who started mostly clueless about 3D scanning, this project gave me insight to a wholly different field of study, and I have come out richer with this experience.

18.2 Ahmed Azeem

Initially it was my belief that design and innovation are the only fundamentals for a good product. However, this was the result of my ignorance and lack of experience in the many stages required to convert a design into a sustainable product for human use. This project was a deep insight into the constraints emerging during manufacturing, safety analysis, budget and the clientele. These tended to be well connected and finding the right balance satisfying all was the true challenge faced within this project. A viable project requires a viable design that takes into consideration all its future stages, alongside its associated limitations, beforehand and incorporates these within the design. Continuous iteration between future stages and the design stage may seem reasonable however, in an environment with restricted resources (i.e. time, finance, etc.) it is vital that design feasibility is considered in the first instance of the project. Such were the ponderings of initially belittling a simple transmission assembly.

I was mainly responsible for manufacturing, budgeting and procurement. These tasks gave me an insight into the restrictions they placed on design and thus indicated the importance of planning and project experience. The team consisted of a series of personalities including coordinator, shaper, monitor evaluator, completer finisher, etc. Such a blend of personalities allowed the project to stay on track and achieve the high standards set by our client.

The software aspect of the project was unconventional for most of us thus pushing us out of our field of expertise. It was vital to maintain focus on that which was necessary and not get

lost in the minute details of the complexities involved. I personally not having a significant involvement on the software aspect preferred to evaluate it as a black box with inputs and outputs connecting it to the rest of the system.

Overall, it was a great experience working alongside a team of disciplined and keen individuals who manifest the high standard of students this college enrolls.

18.3 Jeremy Tan

Dynoscan 3D was not a traditional mechanical project, and because of that it has been an intellectually stimulating process. While a lot of technical difficulties and setbacks were encountered along the way, in retrospect these were the biggest learning points for me to develop a better approach to problem solving. I felt that being able to work through challenging design problems very early on into the project, by having honest discussions, set a positive tone and atmosphere for group work. It was enjoyable to work with group mates who did not shy away from taking initiative or challenging each other's reasoning to ensure the best outcome was delivered.

Being interested in how to manage projects, I was happy to take on the role of project manager. Initially I found it very difficult to establish a sequential timeline with specific deadlines to meet because this was a non-traditional mechanical engineering project, due to a significant portion being software related. Part of the difficulty and cause of stress was due to an unwillingness to accept that there will always be changes to the project timeline. However, once I embraced that there will always be disruptions regardless of how well planned the project is, it made me more responsive to changes. This was especially true for the unique circumstances that Covid-19 thrust upon us during the later half of spring term. During the first half of the project, I was heavily involved in the designing of the transmission subassembly but felt that I was lacking interaction on the software aspect of the project. I'm glad that I took the opportunity during the second term to get exposure to how the point cloud aligning software works as well as seeing how the image acquisition process works. Being able to have seen both aspects of the project be developed allowed me to better gauge the overall progress of the project and any potential issues that may arise. If I were to do this project again, I think it would be beneficial for there to be more overlap in terms of work scope so that other team members have a better technical understanding of how the entire scanning system functions.

While DMT is an inherently technical project, I felt that the bulk of the learning I took away from this experience was interpersonal and relevant for making me a better team member for future projects. Due to the nature of our DMT project being a product that the client actually

has needs for and will use, I developed a stronger appreciation for how to direct client/supervisor meetings. Initially in the brainstorming and idea generation phase of the project, it was difficult to commit to an idea especially when new, albeit useful, suggestions were raised at every meeting, which ultimately delayed decision making and design progress. I personally found it challenging during that period to keep myself from mentally comparing our group progress to other groups, given that our project fundamentally had a different timeline due to the extensive involvement of software in the project. Therefore, managing the expectations of the team and the supervisors/clients as well as getting them to agree on a proposed idea was a process that I had to learn on the go.

18.4 Hussain Siddiquey

Just a few months ago, I had no understanding of 3D scanning at all yet we have managed to create a product capable of scanning an object and generating a 3D model. I chose this project because of my interest in robotics and programming and it was a rewarding experience to work alongside talented but more importantly dedicated individuals. This project would not have been a success had it not been for the combined effort of each of my group members, who have worked hard and supported each other throughout the year.

The main challenge of this project has been selecting a scanning method that would meet the accuracy requirements of the Dynamics Group given the mechanical, software and budget constraints. Initial stages of development were taken up mainly by extensive research into the various scanning methods followed by multiple design iterations based on supervisors' feedback. At times, I had concerns about whether the project was progressing at the correct pace but I was impressed by the balance between the group's delegation of roles, which made individuals responsible for completing their tasks in a timely manner, and the willingness to help beyond our respective job roles, thus ensuring that deadlines were always met. Group members communicated effectively so that everyone was aware of the current stage of development and could discuss any issues that were encountered. When it came to administration, I played the role of secretary and was tasked with keeping a track of the work carried out by each member and recording all things discussed during meetings so that anything said or done could be referenced accurately. Having a detailed account of the meeting minutes made it easy to understand why certain decisions were made which helped when writing the final report.

As the analysis lead, I was responsible for assessing the suitability of a concept or component and integrating it with the overall design. More specifically, I helped select a transmission system and support mechanisms to ensure that the scanner was structurally sound under

various loading conditions while maintaining portability. I was also heavily involved with the motor selection so it was to my disappointment that the motor failed to rotate the turntable during prototype testing. This taught me that there are certain factors that are difficult to predict theoretically and therefore highlighted the importance of empirical testing.

Due to the Covid-19 pandemic, the final product could not be tested which would have been a chance to see the culmination of everyone's hard work. My only regret, however, is not working on the software and electronics more. While my involvement may not have been necessary, it would have been an interesting learning experience that helped me develop a different set of skills. Nevertheless, I am proud of what we have achieved and believe that the scanner can now serve as a stepping stone for further improvement.

18.5 Chuan Sheng Tiong

The journey to design and manufacture Dynoscan has been challenging and rewarding. I chose this DMT project as the idea of extracting 3D profiles from actual objects was interesting and I am proud of what we had achieved despite the challenges. Although we did manage to manufacture our product, it is slightly regrettable that we did not get to test it in its entirety due to Covid-19. Every member of the team has been dedicated to the project and as a team, we have communicated and worked effectively together by playing to our individual strengths.

Due to nature of our project, there were more focus on the software and controls aspects. Having an interest in software and electronics, I was assigned to be the electronics and controls lead. My responsibilities were to design an electronic control system for the turntable and also to integrate the control system with the scanning software so that the turntable rotates the object when the user starts the scan. Although I took the module Embedded C in Microcontrollers, it was not particularly useful as the hardware and system we adopted were different, but the module did teach me some good practices for coding which was helpful. As such, further research was required to find the optimal solution for our turntable and the solution must be implementable by us. Being involved in the electronics and controls aspect of the design, I was quite isolated from the other aspects such as mechanical analysis and software design for the scanning device. Although all aspects of the design were discussed and explained, there was still some lack of depth in understanding for some aspects. I feel that this was unavoidable due to the timeline and workload of the project but given the opportunity, I would have liked to contribute more towards the mechanical design and also the development of the software for the scanning device.

Tasked with the administrative role of liaising with the supervisors and any relevant parties, I learnt that communication is crucial as it clarifies objectives and expectations. This also ensured that we were clear about what we had to do along the whole DMT project. I have not undertaken a similar role like this before and I have learnt how to communicate effectively.

Throughout DMT, we have gone through several iterations of our design to improve and finalise our design. This helped me realise the imperative process of iterative design. It is also important to set realistic targets so that we have the capacity to achieve them. Although we have completed our design and I am contented with our product and our process, there are always still areas for improvement. As modularity is also incorporated into our design, I hope that this project can be developed further and be used in practical applications.